THERMOCATALYTIC CO_2-FREE PRODUCTION OF HYDROGEN FROM HYDROCARBON FUELS

Final Report for the Period
August 1999 – September 2000

Nazim Muradov, Ph.D.

FLORIDA SOLAR ENERGY CENTER
UNIVERSITY OF CENTRAL FLORIDA

Date Published - October 2000

PREPARED FOR THE UNITED STATES
DEPARTMENT OF ENERGY
Under Cooperative Agreement:
No. DEFC3699G010456

DISCLAIMER

DISCLAIMER

Portions of this document may be illegible in electronic image products. Images are produced from the best available original document.

CONTENTS

LIST OF FIGURES

LIST OF TABLES

EXECUTIVE SUMMARY

This report is an account of the work performed at the Florida Solar Energy Center (FSEC) under the Cooperative Agreement No. DE-FC36-99G010456 (U.S. Department of Energy) on the project entitled "Thermocatalytic CO_2-free Production of Hydrogen from Hydrocarbon Fuels".

Objectives: The overall objective of this work is to develop a novel process for CO_2-free production of hydrogen via thermocatalytic decomposition (pyrolysis) of hydrocarbon fuels as a viable alternative to the conventional processes of methane steam reforming or partial oxidation. The objective of Phase I work was to demonstrate the technical feasibility of CO_2-free production of hydrogen and carbon from different hydrocarbons, including methane, propane and gasoline.

Approach: The technical approach is based on a single-step decomposition (pyrolysis) of hydrocarbons over carbon catalysts in air/water free environment. This approach eliminates the need for water-gas shift reactor, CO_2 removal, and the catalyst regeneration, which significantly simplifies the process. Clean carbon is also produced as a valuable byproduct of the process.

Results: The following is the summary of experimental results:

- The technical feasibility of CO_2-free production of hydrogen via thermocatalytic decomposition (TCD) (or pyrolysis) of different hydrocarbons was demonstrated. Methane, propane and gasoline were efficiently converted into hydrogen-rich gas and carbon using selected carbon catalysts.
- The catalytic activity and stability of more than 30 different forms and modifications of carbon were examined, and most promising carbon catalysts were selected for further evaluation.
- The effect of the operational parameters and hydrocarbon nature on the hydrogen yield was determined. Depending on the above factors, hydrogen concentration in the effluent gas varied in the range of 30-90 v.%, balance- CH_4 and small amount of C_2+ hydrocarbons. No CO or CO_2 was detected among the reaction products.
- The factors controlling carbon catalyst activity and long term stability were studied. It was found that the surface area and crystallographic structure mostly determined the catalytic activity of carbon catalysts. This was confirmed by XRD and SEM studies of carbon catalysts.
- It was discovered that the sustainable production of hydrogen-rich gas could be attained by combination of certain types of carbon catalysts, process flow arrangement and operational conditions. Based on these experimental findings the U.S. Patent Application No. 60/194828 was filed.
- A kinetic model for methane decomposition reaction over carbon catalysts was developed. Major kinetic parameters of methane decomposition reaction (rate constants, activation energies, etc.) over selected carbon catalysts were determined. Intermediate and final products of methane and propane pyrolysis were identified and quantified.
- Various conceptual designs for the hydrocarbon pyrolysis reactor, including packed bed, tubular, free volume, fluid wall and fluidized bed reactors, were evaluated; the experimental reactors for decomposition of methane were fabricated and tested. Advantages and disadvantages of each type of the reactor were assessed.

- A bench-scale fluidized bed, packed bed and tubular reactors were designed, fabricated and tested. Simultaneous production of hydrogen-rich gas and carbon was demonstrated using methane, propane and gasoline as feedstocks.
- Preliminary techno-economic assessment of the TCD process indicates that the thermocatalytic unit with the capacity of an average steam reforming (SR) plant would yield hydrogen at a cost of $5.0/MMBTU (if carbon is sold at $100/t), which is less than that for SR process. It was estimated that the TCD process compares favorably with SR coupled with CO_2 sequestration even if carbon is not sold, but stored for future use.
- Comparative assessment of CO_2 emissions from different hydrogen production processes clearly demonstrated the significant ecological advantages of the TCD process over conventional processes.

1. INTRODUCTION

Given the advantages inherent in fossil fuels, such as their availability, cost-competitiveness, convenience of storage and transportation, they are likely to play a major role in hydrogen production for the 21st century. In principle, hydrogen can be produced from hydrocarbon fuels (e.g. natural gas, NG) by reaction with water, oxygen, water/oxygen, and decomposition:

1. Reaction with water (steam reforming, SR):

$$CH_4 + 2H_2O \rightarrow 4H_2 + CO_2$$

2. Reaction with oxygen (air) (partial oxidation, POx):

$$CH_4 + O_2 \rightarrow 2H_2 + CO_2$$

3. Reaction with water and oxygen (air) (autothermal reforming, ATR):

$$CH_4 + H_2O + 1/2O_2 \rightarrow 3H_2 + CO_2$$

4. Methane decomposition reaction:

$$CH_4 \rightarrow 2H_2 + C$$

First three approaches produce large amounts of CO_2: up to 0.25-0.33 m^3 CO_2 per m^3 of H_2 produced. For example, a typical hydrogen plant with the capacity of approximately one million m^3 of hydrogen per day produces about 0.25 million standard cubic meters of CO_2 per day (exclusive of stack gases), which is normally vented into the atmosphere.

There are several possible ways to mitigate CO_2 emission problem. Among them are traditional (e.g. more efficient use of fossil fuel energy resources; increase in usage of non-fossil fuels, etc.) as well as the approaches which include sequestration of CO_2 produced by the conventional processes. The perspectives of CO_2 sequestration is actively discussed in the literature. The main objective of carbon sequestration is to prevent anthropogenic CO_2 emissions from reaching the atmosphere by capturing and securely storing CO_2 underground or under the ocean. However, there are some environmental uncertainties associated with CO_2 sequestration.

A novel approach to hydrogen production without CO_2 emissions is related to decomposition of NG (or other hydrocarbon fuels) into hydrogen and carbon. This process is much less developed comparing to the conventional processes of SR and POx. Thus, the main objective of this work is to develop the thermocatalytic process for CO_2-free production of hydrogen and carbon from methane and other hydrocarbon fuels. Another objective is to compare the thermocatalytic process with methane steam reforming process coupled with CO_2 sequestration.

If cost effective CO_2-free hydrogen production technologies are developed and implemented, there would be practically no environmental constraints on using fossil fuels on a large scale for the foreseeable future.

2. TECHNICAL BACKGROUND

2.1. Conventional Processes of Hydrogen Production

2.1.1. Steam Reforming of Methane

For decades, steam reforming of methane (or NG) has been the most efficient and widely used process for the production of hydrogen. Typical capacities of SR plants are in the range of hundreds of thousands of cubic meters per hour of hydrogen, which makes them most economical among all hydrogen producing technologies. The process basically represents a catalytic conversion of methane (a major component of the hydrocarbon feedstock) and water (steam) to hydrogen and carbon oxides, and consists of three main steps:

a) steam reforming: $CH_4 + H_2O \rightarrow CO + 3H_2$ $\Delta H^o = 214.5$ kJ/mol

b) water-gas shift reaction: $CO + H_2O \rightarrow CO_2 + H_2$ $\Delta H^o = -41.5$ kJ/mol

c) gas purification (CO_2 removal)

Overall: $CH_4 + 2H_2O \rightarrow CO_2 + 4H_2$ $\Delta H^o = 173.0$ kJ/mol

Four moles of hydrogen are produced in the reaction with half of it coming from the methane and another half from water. The theoretical energy requirement per mole of hydrogen produced for the overall process is equal to 173/4= 43.3 kJ/mole H_2. To ensure a maximum conversion of CH_4 into the products, the process generally employs a steam/carbon ratio of 3÷5, the process temperature of 800-900°C and pressure of 35 atm [1]. The SR process thermal efficiency is seldom greater than 50% [1]. A steam reformer fuel usage is a significant part (up to 30-40%) of the total NG usage of a typical hydrogen plant. The typical composition of a synthesis gas after the reformer is (expressed in v.%): H_2- 74, CO- 18, CO_2- 6, CH_4- 2. After two stages (high and low temperature) of water gas shift conversion the concentration of CO usually drops to 0.4 v.%. Finally, the raw gas passes a series of gas purification units, first, to remove bulk of CO_2 and then to remove the residual CO and CO_2. The average purity of H_2 after these stages is 97-98 v.%. Hydrogen at 99.99 v.% purity can be obtained after additional purification using a pressure swing adsorption (PSA) unit. There is no by-product credit for the process and, in the final analysis, it does not look environmentally benign due to large CO_2 emissions The total CO_2 emission from SR process reaches up to 0.35-0.42 m^3 per each m^3 of hydrogen produced.

2.1.2. Partial Oxidation

Partial oxidation (POx) of NG (catalytic and non-catalytic) can be described by the following equations:

$CH_4 + 1/2O_2 \rightarrow CO + 2H_2$ $\Delta H^o = -35.6$ kJ/mol

$CH_4 + O_2 \rightarrow CO_2 + 2H_2$ $\Delta H^o = -319.3$ kJ/mol

$$CO + H_2O \rightarrow CO_2 + H_2 \qquad \Delta H^o = -41.5 \text{ kJ/mol}$$

2--3 moles of hydrogen are produced per one mole of methane. Both reactions are exothermic which implies that the reactor does not need an external heat source. If pure oxygen is used in the process, it has to be produced (or purchased) and stored which significantly adds to the cost of the system. On the other hand, if POx process uses air as an oxidizer, the effluent gas is heavily diluted by nitrogen which results in larger water gas shift reaction (WGSR) and gas purification units. The maximum theoretical concentration of hydrogen in the effluent gas using pure oxygen is 66.7 v.%, however, the concentration drops to 40.9 v.% if air is used as an oxidizer.

$$CH_4 + 1/2(O_2 + 79/21)N_2 \rightarrow 2H_2 + CO + 79/42N_2 \qquad \Delta H^o = -35.6 \text{ kJ/mol}$$

POx process has a number of important advantages over SR:

- it provides a simplified system due to absence of external water and heat supply, therefore, it is potentially less expensive,
- POx reactor potentially has the capability to process a variety of gaseous and liquid hydrocarbon fuels including methane, LPG, gasoline, diesel fuel, methanol, etc.,

However, POx process also suffers from the following disadvantages:

- POx reformate, which is heavily diluted with nitrogen, has lower calorific value,
- since POx process is exothermic and involve significantly higher temperatures, it might have greater thermal loses,

2.1.3. Autothermal Reforming

In autothermal reforming (AR) process hydrocarbon fuel reacts with a mixture of water and oxygen:

$$2C_nH_{2n+2} + n/2O_2 + nH_2O \rightarrow 2nCO + (3n+2)H_2$$

$$C_nH_{n+2} + n/2O_2 + nH_2O \rightarrow nCO_2 + (2n+1)H_2$$

The energy released by hydrocarbon oxidation reaction drives steam reforming process. The overall process is exothermic and it features almost the same advantages and disadvantages of POx process, although, AR produces somewhat more hydrogen per unit of hydrocarbon fuel consumed relative to POx. Rolls-Royce/Johnson-Mathey and International Fuel Cell/ONSI have been working on the development of the autothermal reformer units [2].

2.1.4. Steam-Iron Process

There have been attempts to produce high-purity hydrogen from hydrocarbons by modification of well known steam-iron process. For example, in a process developed by H Power Corp.

(U.S.A.) sponge iron is oxidized in multiple bed reactor to provide high-purity hydrogen to a fuel cell, while already depleted beds are regenerated (reduced) using synthesis gas delivered from a methane-fueled steam reformer (or PO unit):

$3Fe + 4H_2O \rightarrow Fe_3O_4 + 4H_2$ $\Delta H^o = -151.3$ kJ/mol (Fe_3O_4)

$Fe_3O_4 + 4CO \rightarrow 3Fe + 4CO_2$ $\Delta H^o = -14.7$ kJ/mol (Fe_3O_4)

$Fe_3O_4 + 4H_2 \rightarrow 3Fe + 4H_2O$ $\Delta H^o = 151.3$ kJ/mol (Fe_3O_4)

The advantage of this process is that it produces very pure hydrogen without energy- and material-intensive stages of hydrogen purification (e.g. WGSR and CO_2 removal). However the process is multistage, requires high temperatures (for the reduction of magnetite, Fe_3O_4, to sponge iron) and additional step of NG steam reforming (or POx). In a vehicle application, authors suggest that a 113 kg bed of sponge iron granules placed in a car which will react with a steam to produce hydrogen for fuel cell or internal combustion engine [3]. The spent iron oxide will be blown out of the bed with air pressure and sent off for the regeneration (reduction) in a stationary unit, and a replacement dose of fresh sponge iron will be pumped in. According to the stoicheometry of the iron-steam reaction, the production of 1 m^3 of hydrogen requires 2.1 kg of sponge iron and 0.75 kg of H_2O. Considering that at least a two- or tree-fold surplus of water will be required to enhance the kinetics of the reaction and bring it to completion, the total weight of the reagents on board would be 3.6-4.4 kg per 1 m^3 of hydrogen produced (not accounting the fuel required for start-up). Calculations show that in order to supply 20 kW fuel cell with pure hydrogen obtained from 113 kg of sponge iron one needs to regenerate iron oxide bed every 2 hours of driving, thus, almost every day. The theoretical yield of hydrogen is 3 moles H_2 per mole of CH_4, which in real systems will be significantly less due to heat losses and consumption of methane as a heat source.

2.2. CO_2 Sequestration

The perspectives of CO_2 sequestration is actively discussed in the literature, e.g. [4]. The main objective of carbon sequestration is to prevent anthropogenic CO_2 emissions from reaching the atmosphere by capturing and securely storing CO_2 underground or under the ocean. Of particular interest is the sequestration of CO_2 produced by the conventional hydrogen production processes (e.g. SR, PO). If these hydrogen production technologies could be coupled with CO_2 sequestration, there would be practically no environmental constraints on using fossil fuels on a large scale. A typical hydrogen plant with the capacity of approximately one million m^3 of hydrogen per day produces about 0.25 million standard cubic meters of CO_2 per day (exclusive of stack gases), which is normally vented into the atmosphere. CO_2 concentrations in process streams range from approximately 5 v.% for stack gases to almost 100 v.% for concentrated streams after pressure swing adsorption (PSA) unit (or other advanced gas separation systems). The present-day options for CO_2 capture and separation include:

- absorption (chemical and physical),
- adsorption (chemical and physical),
- low-temperature distillation and

- membrane separation.

Since all stages of CO_2 sequestration process, including its capture, pressurization, transportation and injection underground (or under the ocean) are energy intensive processes, it was important to estimate the total energy consumption per unit of CO_2 sequestrated. The following summarizes available data on the energy consumption during CO_2 sequestration associated with the SR process (per kg of sequestrated CO_2):

- CO_2 capture by hot K_2CO_3 solutions, ~3000 kJ, [5]
- CO_2 pressurization to 80 bar by 5 stage compression, 281 kJ_{el}, [6]
- CO_2 pipeline transportation for 100-500 km to the disposal site and injection, ~2000 kJ

About 80% of the world's commercial energy is based on fossil fuels [4]. World average for CO_2 emission associated with the electricity production is 0.153 kg of CO_2 per each kWh produced [6]. Thus, the total CO_2 emissions from CO_2 sequestration are estimated at 0.20-0.25 kg CO_2 per kg of sequestrated CO_2. Apparently, CO_2 sequestration is an energy intensive process and, in the final analysis, does not completely eliminate CO_2 emission. In addition to this problem, some uncertainties remain regarding the duration and extent of CO_2 retention (underground or under the ocean) and its possible environmental effect.

There have been some estimates reported in the literature on the economics of CO_2 sequestration associated with hydrogen production from fossil fuels. Thus, according to authors [7], the capture and disposal of CO_2 (80-85% of CO_2 captured from the concentrated streams of SR process) add about 25-30% to the cost of hydrogen produced by the SR of NG. The capture and disposal of CO_2 from diluted stack gases is even more costly. For example, it was estimated that the cost of eliminating CO_2 emissions from stack gases of advanced power generation plants range from $35 to 264 per ton of CO_2 [8]. Thus, CO_2 sequestration is an energy intensive and expensive process and, in the final analysis, does not completely eliminate CO_2 emission. In addition to this problem, some uncertainties remain regarding the duration and extent of CO_2 retention (underground or under the ocean) and its possible environmental effect.

2.3. Production of Hydrogen by Methane Decomposition

2.3.1. Thermal Decomposition of Methane

Thermal decomposition (TD) of methane produces hydrogen and carbon as expressed by the following chemical equation:

$$CH_4 \rightarrow C + 2H_2 \qquad \Delta H^\circ = 75.6 \text{ kJ/mol}$$

The energy requirement per mole of hydrogen produced (37.8 kJ/mole H_2) is somewhat less than that for the SR process. The process is slightly endothermic so that less than 10% of the heat of methane combustion is needed to drive the process. In addition to hydrogen as a major product, the process produces a very important by-product: clean carbon. The process is environmentally compatible, as it produces relatively small amounts of CO_2 (approximately 0.05 m^3 per m^3 of H_2 produced, if CH_4 is used as a fuel). It should be noted, however, that the process

could potentially be completely CO_2-free if a relatively small part of hydrogen produced (approximately 14%) is used as a process fuel.

TD of NG is a technologically simple one-step process and, unlike SR and POx, it does not require several expensive technological steps such as WGSR, CO_2 removal, oxygen production, steam generation and excess steam removal (drying). A preliminary process design for a continuous methane decomposition process and its economics have been conducted [9]. The techno-economic assessment showed that the cost of hydrogen produced by TD of NG ($58/1000 m^3 H_2, with carbon credit), was somewhat lower than that for the SR process ($67/1000 m^3 H_2) [9]. It should be noted that the capital cost component of the production cost for TD process (before carbon credit) is equal to 12.8% comparing that to 29.1 and 47.9% for SRM and POx, respectively [9].

2.3.2. Advanced Processes of Methane Decomposition

Methane is one of the most stable organic molecules. Its electronic structure, lack of polarity and any functional group makes it extremely difficult to decompose methane molecule into its constituent elements. Recently, several new approaches to methane decomposition were reported in the literature.

2.3.2.1. Advanced Thermal Systems

The authors [10] proposed a methane decomposition reactor consisting of a molten metal bath. Methane bubbles through molten tin or copper bath at high temperatures (900°C and higher). The advantages of this system are: an efficient heat transfer to a methane gas stream and ease of carbon separation from the liquid metal surface by density difference. In another work [11], methane decomposition was carried out in a continuous process using a metallic tubular reactor in the range of temperatures 700-900°C and pressures 28.2-56.1 atm. It was shown that at 900°C, 56.1 atm and sufficiently high residence time (>100 sec.) the concentration of methane in the effluent gas appeared to be approaching the equilibrium conditions. The determined reaction activation energy of E_a= 131.1 kJ/mol, was substantially lower than E_a reported in the literature for homogeneous methane decomposition (272.4 kJ/mol) which pointed to a significant contribution of the heterogeneous processes caused by the submicron size carbon particles adhered to the reactor surface. A high temperature regenerative gas heater (HTRGH) for hydrogen and carbon production from NG has been developed [12]. In this process thermal decomposition of NG was conducted in "free volume" of HTRGH using carrier gas (N_2 or H_2) which was pre-heated up to 1627-1727°C in the matrix of the regenerative gas heater. The reactor was combined with a steam turbine to increase the overall efficiency of the system.

2.3.2.2. Plasma Decomposition

Plasma-assisted decomposition of hydrocarbons with the production of hydrogen and carbon has become an active area of research recently. Kvaerner company of Norway has developed a methane decomposition process which produces hydrogen and carbon black by using high temperature plasma (CB&H process) [13]. The advantages of thermal plasma process are: high thermal efficiency (>90%), high fuel flexibility, purity of hydrogen (98 v.%) and production of

valuable byproduct- carbon. The authors claim very low CO_2 emissions associated with the plasma process.

In the paper [14], the authors advocated a plasma-assisted decomposition of methane into hydrogen and carbon. It was estimated that 1-1.9 kWh of electrical energy is consumed per one normal cubic meter of hydrogen produced. The authors stated that plasma production of hydrogen is free of CO_2 emissions. However, since most of the electric energy supply in the world comes from fossil fuels, the electricity-driven hydrogen production processes, including plasma and electrochemical processes, are among CO_2 producers.

2.3.2.3. Photolysis

Due to high dissociation energy of CH_3 - H bond (D_o= 4.48 eV) methane absorbs irradiation in vacuum ultra-violet region. The absorption spectrum of methane is continuous in the region from 1100 to 1600Å (absorption coefficient k= 500 $atm^{-1}cm^{-1}$ at 1100-1300Å). Unfortunately, the wavelengths shorter than 1600 Å are present neither in the solar spectrum, nor in the output of most UV lamps. Therefore, production of hydrogen and other products by direct photolysis of methane does not seem to be practical.

Methane molecule could be activated in the presence of special photocatalysts using near-UV photons which are present in the solar spectrum (up to 5% of total energy). Previously we have demonstrated photocatalytic conversion of low alkanes (C_1-C_3) to unsaturated hydrocarbons (mostly C_2-C_4 olefins) under UV irradiation using polyoxometalates of W, Mo, V and Cr [15]. The diffuse reflectance UV-VIS spectra of the synthesized silica-supported polyoxotungstates (POT, $[H_xW_yO_z]$) exhibit a continuous absorption up to 350 nm (near-UV area). Irradiation of methane adsorbed to the surface of POT/SiO_2 with near-UV photons at room temperature resulted in the photoreduction of POT to its reduced (blue-colored) form with simultaneous photoconversion of methane to C_2^+ products. Thermal desorption (125-200°C) of products in vacuum resulted in the following gaseous mixture (v.%): C_2H_4- 40.2, C_3H_6- 21.7, C_4H_8- 36.0, C_5^+- 2.1. CO and CO_2 were not detected among the products of methane photo-transformation. The total products yield (per adsorbed methane) was 17%, however, doping the POT catalyst with Pt (0.1 w.%) increased the products yield to 32.1%. In the presence of UV-illuminated SiO_2-supported (5 w.%) silica-tungstic acid ($H_4SiW_{12}O_{40}$) 19.3% of the adsorbed methane was converted to the following gaseous mixture (v.%): C_2H_4- 4.1, C_3H_6- 7.3, C_4H_8- 86.2, C_5^+- 2.4.

The mechanism of methane photoactivation involves the initial photoinduced charge transfer in photoactive W^{6+}=O groups of POT and STA molecules, leading to the formation of very active electron-deficient species able to abstract H-atom from methane molecule:

$$W^{6+}=O + h\nu \rightarrow W^{5+}\text{-}O^{\cdot}$$

$$W^{5+}\text{-}O^{\cdot} + CH_4 \rightarrow W^{5+}\text{-}OH + CH_3^{\cdot}$$

$$W^{6+}=O + CH_3^{\cdot} \rightarrow W^{5+}\text{-}OCH_3$$

$$2W^{5+}\text{-}OCH_3 \rightarrow 2W^{5+}\text{-}OH + (C_2H_4)_{chem}$$

Higher molecular weight olefins (C_3H_6, C_4H_8, etc.), are, most likely, produced by the secondary catalyzed reactions of chemisorbed ethylene, $(C_2H_4)_{chem}$. After the photoreaction, the photocatalyst remains in its photoreduced form (W^{5+}-OH) at ambient temperature. It could be thermally regenerated to its initial oxidized form (W^{6+}=O) by releasing hydrogen:

$$2W^{5+}\text{-OH} \rightarrow 2W^{6+}\text{=O} + H_2$$

Thus, the overall reaction represents the photocatalytic transformation of methane to hydrogen and ethylene:

$$2CH_4 + h\nu \rightarrow C_2H_4 + 2H_2$$

Concentrated solar irradiation could be used to drive the thermal stages (desorption of products and regeneration of the catalyst) of this process. The advantage of this potentially solar-driven process is that it converts methane to hydrogen and valuable olefins without production of CO_2.

2.3.2.4. Thermocatalytic Decomposition

There has been attempts to use catalysts in order to reduce the maximum temperature of thermal decomposition of methane. Thus, in 60-s, Universal Oil Products Co. has developed the HYPRO® process for continuous production of hydrogen by catalytic decomposition of a gaseous hydrocarbon streams [16]. Methane decomposition was carried out in a fluidized bed catalytic reactor in the range of temperatures from 815 to 1093°C. Supported Ni, Fe and Co catalysts (preferably, Ni/Al_2O_3) were used in the process. The coked catalyst was continuously removed from the reactor to the regeneration section where carbon was burned off by air, and the regenerated catalyst returned to the reactor. Unfortunately, the system with two fluidized beds and the solids-circulation system was too complex and expensive and could not compete with the SR process.

NASA has conducted studies on the development of catalysts for methane decomposition process for space life support systems [17]. A special catalytic reactor with a rotating magnetic field to support Co-catalyst at 850°C was designed. In 70s, a group of U.S. Army researchers has been developing a fuel processor (conditioner) to catalytically convert different hydrocarbon fuels to hydrogen which was used to feed a 1.5 kW fuel cell [18]. A stream of gaseous fuel entered one of two reactor beds, where hydrocarbon decomposition to hydrogen took place at 870-980°C and carbon was deposited on the Ni-catalyst. Simultaneously, air entered the second reactor where the catalyst regeneration by burning coke off the catalyst surface occurred. The streams of fuel and air to the reactors then were reversed for another cycle of decomposition-regeneration. The reported fuel processor did not require WGS and gas separation stages, which was a significant advantage. However, the thermal efficiency of this type processors, in general, is relatively low (<60%) and they produce CO_2 in quantities comparable with SR and PO processes. Recently, several groups of researchers have reported on the development of hydrocarbon fuel processors for the fuel cells applications using similar concept [19,20].

It was found that almost all transition metals (d-metals) to some extent exhibited catalytic activity toward methane decomposition reaction, and some of them demonstrated remarkably high activity. It should be noted, however, that there is no universal agreement among different groups of researchers regarding the choice of the most efficient metal catalyst for methane decomposition. For example, it was demonstrated [21] that the rate of methane activation in the presence of transition metals followed the order: Co, Ru, Ni, Rh > Pt, Re, Ir > Pd, Cu, W, Fe, Mo. The authors [19,22] have found Pd to be the most active catalyst for methane decomposition, whereas, Ni was the catalyst of choice in the publication [23], and Fe and Ni in publications [24,25]. According to the data presented in [26], Co catalyst demonstrated highest activity in methane decomposition reaction.

Of particular interest are catalytic methane decomposition reactions producing special (e.g. filamentous) form of carbon. For example, the authors [27] have reported catalytic decomposition of methane over Ni catalyst at 500°C with the production of hydrogen and whisker carbon. Concentrated solar radiation was used to thermally decompose methane into hydrogen and filamentous carbon [28]. The advantages of this system include the efficient heat transfer due to direct irradiation of the catalyst and CO_2-free operation.

The nature of methane-metal interaction during decomposition reaction is still debated in the literature. For example, according to [29], the activation energy for methane decomposition is lower for the metals with stronger metal-carbon bonds, which correlates with the following order of activity: Fe > Co > Ni. Our experimental data on methane decomposition over alumina-supported Fe, Ni and Co catalysts at 850°C are in a good agreement with the theory. However at lower temperatures (<700°C) the order of catalytic activity toward methane decomposition changed to Ni > Fe > Co. Apparently, other factors, including hydrogen-metal interaction, also play significant role in methane activation over transition metal catalysts.

No conclusive study is presented in the literature on the mechanism of methane decomposition over metal catalysts. Most likely, a general Langmuir-type mechanism, similar to that suggested for CH_4-D_2 exchange over metal films [30] may be applied to metal-catalyzed methane decomposition reaction:

$$CH_4 + 2^* \rightleftharpoons CH_3^* + H^*$$

$$CH_3 + * \rightleftharpoons CH_2^* + H^*$$

$$CH_2 + * \rightleftharpoons CH^* + H^*$$

$$CH + * \rightleftharpoons C + H^*$$

where, * is an active site.

3. TECHNICAL APPROACH AND OBJECTIVES

3.1. Technical Approach

Our technical approach is based on thermocatalytic decomposition of hydrocarbons over carbon-based catalysts in air/water-free environment. The use of carbon-based catalysts offers the following advantages over metal catalysts:

- no need for the separation of carbon from the catalyst
- no need for the regeneration of the catalyst by burning carbon off the catalyst surface
- no CO/CO_2 production due to the combustion of carbon
- no contamination of hydrogen with carbon oxides and, consequently, no need for the additional gas purification (e.g. via methanation)
- the process could be arranged in a continuous mode similar to the industrial processes of fluid coking or fluid catalytic cracking.

3.2. Objectives

Current year objectives include:

- To demonstrate the technical feasibility of CO_2-free production of hydrogen and carbon via catalytic decomposition of hydrocarbons
- To determine efficient carbon catalysts and conditions for sustainable production of hydrogen-rich gases from different hydrocarbons (methane, propane, gasoline)
- To determine factors affecting catalyst activity and long-term stability
- To evaluate different conceptual designs for the thermocatalytic reactor suitable for simultaneous production of hydrogen and carbon
- To preliminarily estimate economic benefits of producing hydrogen and carbon in comparison with steam reforming coupled with CO_2 sequestration

4. EXPERIMENTAL

4.1. Reagents.

Methane (99.99%v.) (Air Products and Chemicals, Inc.) was used without further purification. Samples of activated carbons, graphites, glassy carbon, synthetic diamond powder, fullerenes, carbon nanotubes and acethylene black were obtained from Alfa Aesar and used without further purification. Barneby Sutcliffe Corp. and Cabot Corp. supplied different CB and AC (coconut) samples, respectively. All carbon samples were used in the form of fine powder (<100μm). Activated alumina samples (Fisher Scientific and Alfa Aesar) were used without further purification.

4.2. Apparatus.

The view of the experimental set-up used for hydrogen production via thermocatalytic decomposition hydrocarbons is presented on Figure 4-1. The set-up consisted of 3 main subsystems: (1) a thermocatalytic reactor (with temperature-controlled electric heater and pre-heater), (2) a feedstock metering and delivery sub-system for gaseous and liquid hydrocarbons, and (3) analytical sub-system.

The catalytic reactors were made out of a fused quartz or ceramic (alumina) in order to reduce the effect of the reactor material on the rate of hydrocarbon decomposition.

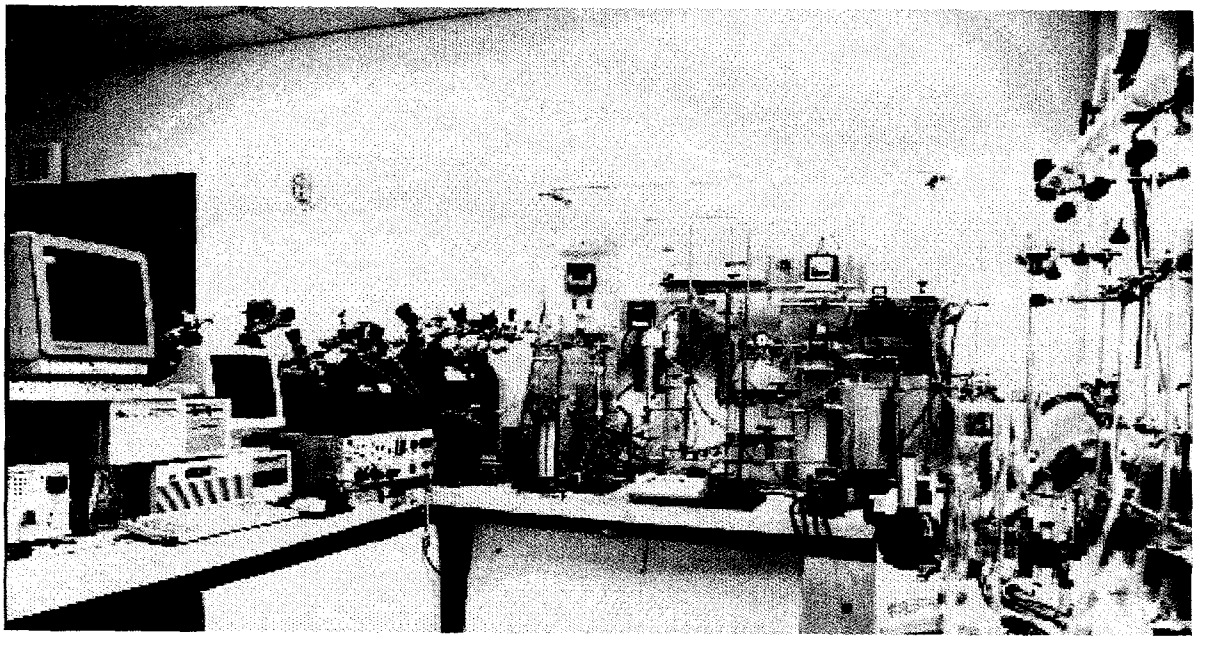

Figure 4-1. FSEC's Experimental Set-up for Thermocatalytic Production of Hydrogen from Hydrocarbons

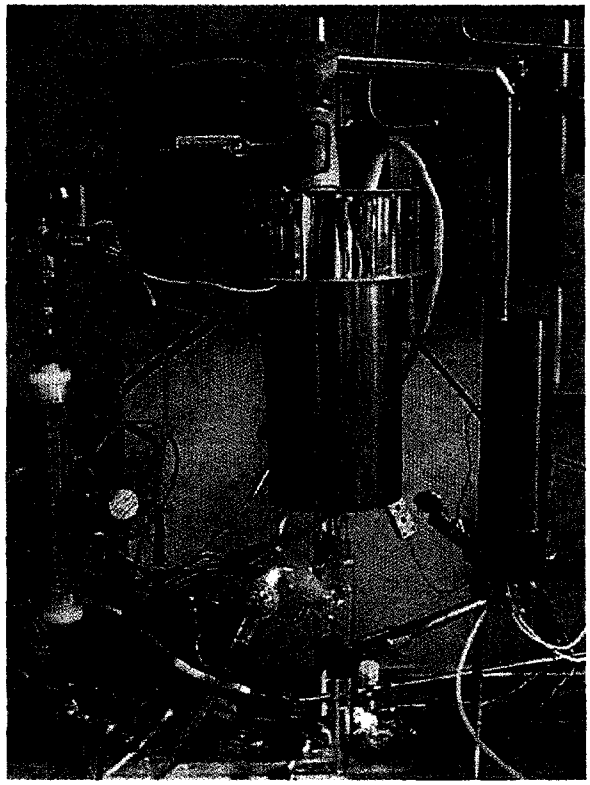

Figure 4-2. Thermocatalytic Reactor with Electric Heaters and a Fuel Evaporator

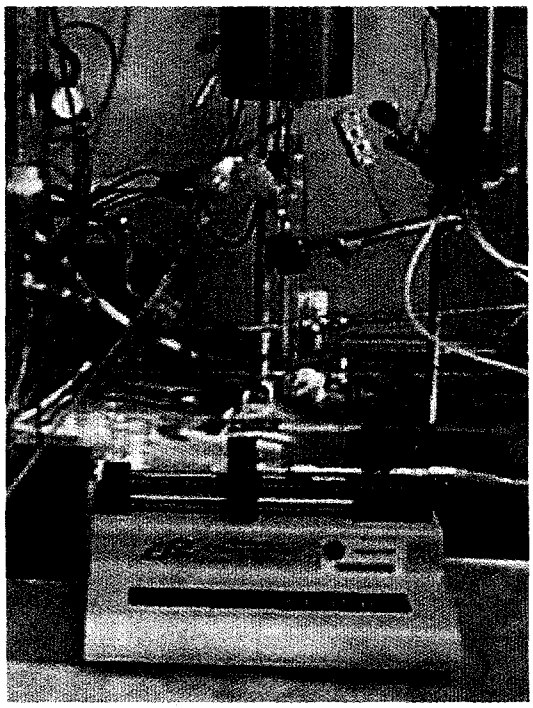

Figure 4-3. Liquid Hydrocarbon Delivery Sub-system

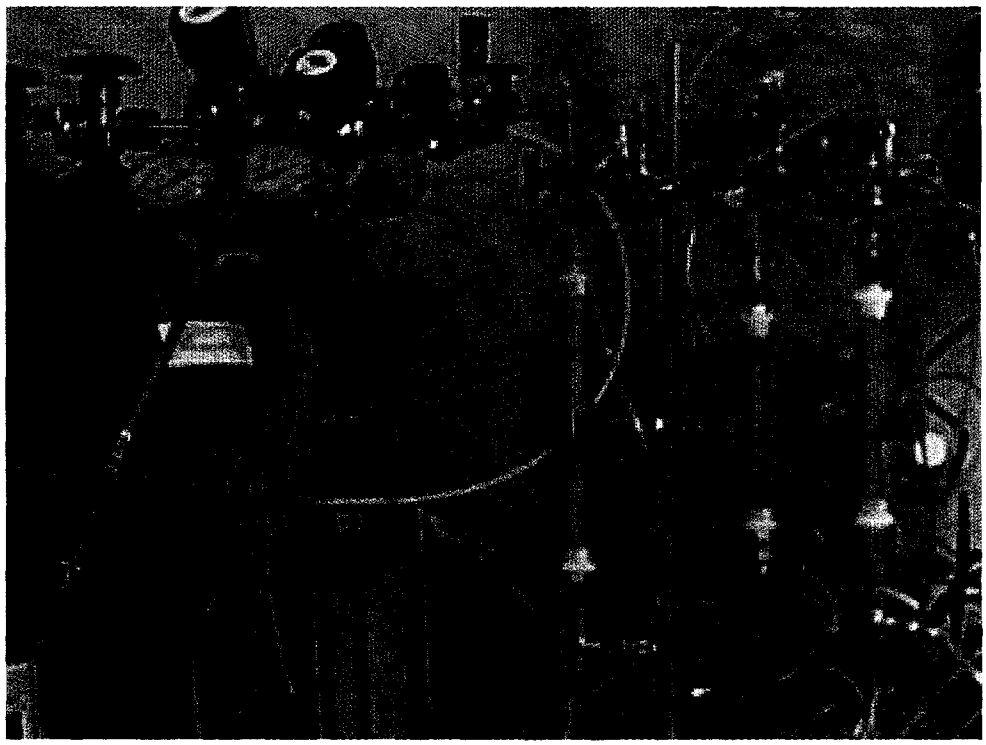

Figure 4-4. Gas Metering and Delivery System

Figures 4-2 through 4-4 demonstrate close views of different sub-systems of the experimental unit:

- a reactor block with an electric heater and pre-heater, and a fuel evaporator
- a liquid hydrocarbon delivery sub-system with a syringe pump
- a gas metering and delivery sub-system

The reactor temperature was maintained at a constant temperature via a type K thermocouple and Love Controls microprocessor. Amount of carbon catalyst used in the experiments varied in the range of 0.03-5.0 g. Gaseous hydrocarbons flow rates varied from 5 ml/min to 2 l/min.

Gaseous hydrocarbons (methane, propane) were metered by flow meters, and liquid hydrocarbons were metered and delivered to the reactor by a syringe pump via a temperature-controlled evaporator. Gaseous products of hydrocarbon decomposition passed through a condenser (for separation of liquid byproducts), a filter (for separation of airborne carbon particles and aerosols) and were analyzed gas-chromatographically .

4.3. Analysis

The analysis of the products of methane decomposition was performed gas chromatographically: SRI- 8610A (a thermal conductivity detector, Ar carrier gas, a silicagel column, temperature programming from 27 to 180°C) and Varian-3400, FID, He-carrier gas, Hysep D_b. SEM studies were performed using Amray 1810 scanning electron microscope. XRD studies were conducted using Rigaku diffractometer with D/MAX 2200T/PC ULTIMA accessory. Polynuclear aromatic byproducts were analyzed spectrophotometrically (Shimadzu UV-2401PC). Carbon particle size and distribution measurements were performed using Model 770 ACCUSIZER (Particle Sizing Systems, Inc.)

5. RESULTS AND DISCUSSION

5.1. *Methane Decomposition over Carbon Catalysts*

We determined the catalytic activity of the variety of carbon-based materials of different structure and origin toward methane decomposition. Table 5-1 summarizes the experimental results of methane decomposition reaction in the presence of different modifications of elemental carbon including wide range of activated carbons (AC), carbon blacks (CB), carbon fiber, glassy carbon, and crystalline graphites, and others, at 850°C and residence time of approximately 1 s. Each carbon sample was characterized by two important parameters: initial activity presented as an initial methane conversion rate, in mmole/min-g (K_m^o) and sustainability displayed in the Table 5-1 as the ratio of methane conversion rate after one hour to the initial methane conversion rate (K_m^1/K_m^o). The available data on the surface area (SA) of carbon samples tested are also presented in the Table 5-1.

It is understood that higher are both K_m^o and K_m^1/K_m^o parameters, better is the carbon catalyst. The experiments indicated that, in general, activated carbons exhibited highest initial activity (per unit of catalyst weight), but relatively low sustainability (K_m^1/K_m^o). It is noteworthy that AC samples of different origin and surface area displayed relatively close initial activity (K_m^o) in the range of 1.6-2.0 mmole/min-g.

Table 5-1. Comparative Assessment of Different Carbon Catalysts in Methane Decomposition Reaction

Carbon Catalyst	SA, m^2/g	K_m^o, mmole/ min-g	K_m^1/K_m^o	Carbon Catalyst	SA, m^2/g	K_m^o, mmole /min-g	K_m^1/K_m^o
AC, Coconut KE	1150	1.76	0.05	Acetylene Black	80	0.22	0.98
AC, Coconut CL	1650	1.67	0.18	CB, Black Pearls	25	0.22	0.48
AC, Coconut GI	1300	1.90	0.07	CB, Regal 330	94	0.42	0.40
AC, Hardwood	1500	2.04	0.32	CB, Vulcan XC72	254	0.48	0.41
AC, G-60	900	1.63	0.28	CB, Black Pearls	1500	1.15	0.60
AC, Lignite	650	1.77	0.31	Glassy Carbon	-	0.95	0.06
AC, Peat RO	900	1.63	0.19	Diamond Powder	-	0.16	0.48
AC, petrol. coke	-	1.29	0.47	Carbon FibersPAN	-	0.05	0.50
Graphite, natural	4-6	0.02	2.87	Carbon Nanotubes	-	0.08	0.92
Graphite, crystal.	3-10	0.10	0.63	Soot (Fullerene)	-	1.90	0.63
Graphite, crystal.	10-12	0.07	0.82	Fullerenes $C_{60/70}$	-	1.34	0.11

Carbon black catalysts (including acetylene black) exhibited somewhat lower initial activity than AC, but better sustainability. Carbons with the ordered structure (graphite, diamond, carbon fiber) demonstrated the lowest initial activity toward methane decomposition reaction.

Fullerenes $C_{60/70}$ and fullerene soot displayed relatively high initial activity, whereas, multi-walled carbon nanotubes showed very low catalytic activity in methane decomposition.

It was found that besides the nature of carbon material, its relative catalytic activity in methane decomposition reaction was proportional to the surface area of carbon. Figure 5-1 depicts the methane conversion rate (in mmole/min-g) as a linear function of the surface area of carbon catalysts in semi-log coordinates. The plot includes data for all the modifications of carbon tested, including AC, CB, graphites and others. It should be noted that only limited number of carbon catalysts could be compared based on the unit of surface area. For example, activated carbon (KBB) produced from hardwood (with SA=1500 m^2/g) demonstrated the initial methane conversion rate of 1.36 μmole/min-m^2, comparing to 0.77 μmole/min-m^2 for carbon black (BP-2000) with the same surface area.

Figure 5-2 (a) demonstrates the kinetic curves of methane decomposition over different types of AC, CB and graphite at 850°C and different residence times. It can be seen that at comparable conditions AC catalysts have higher initial activity than CB catalysts, although, CB-catalyzed decomposition of methane is more sustainable than AC-catalyzed. At relatively high residence times AC catalysts produced H_2/CH_4 mixtures with the initial hydrogen concentrations reaching up to 90 v.% and higher, which is an indication of the high catalytic activity. This, however, was followed by the rapid drop in the catalytic activity and the decrease in methane decomposition rate. CB-catalyzed methane decomposition reached quasi-steady state rate over 20-30 min and remained practically stable for several hours, followed by the gradual decline in the reaction rate.

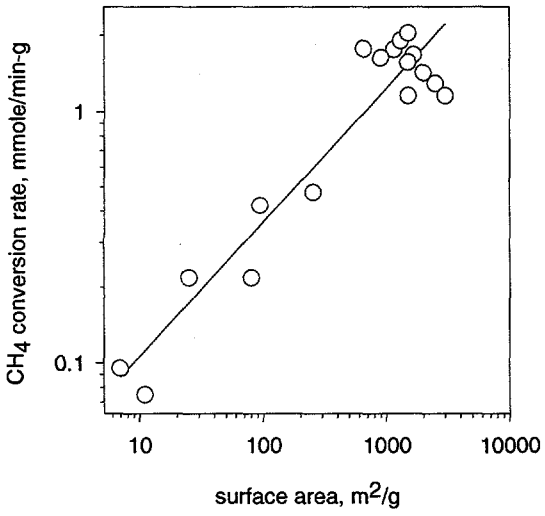

Figure 5-1. Methane Conversion Rate as a Function of Catalyst Surface Area

The initial rate of methane decomposition over amorphous carbons (e.g. acetylene black and carbon blacks) was relatively low, but the process demonstrated good sustainability over long period of time. Figure 5-3 (left) demonstrates the kinetic curves of methane decomposition over acetylene black which was conducted at 850°C and residence time of 12 s for almost 24 hours.

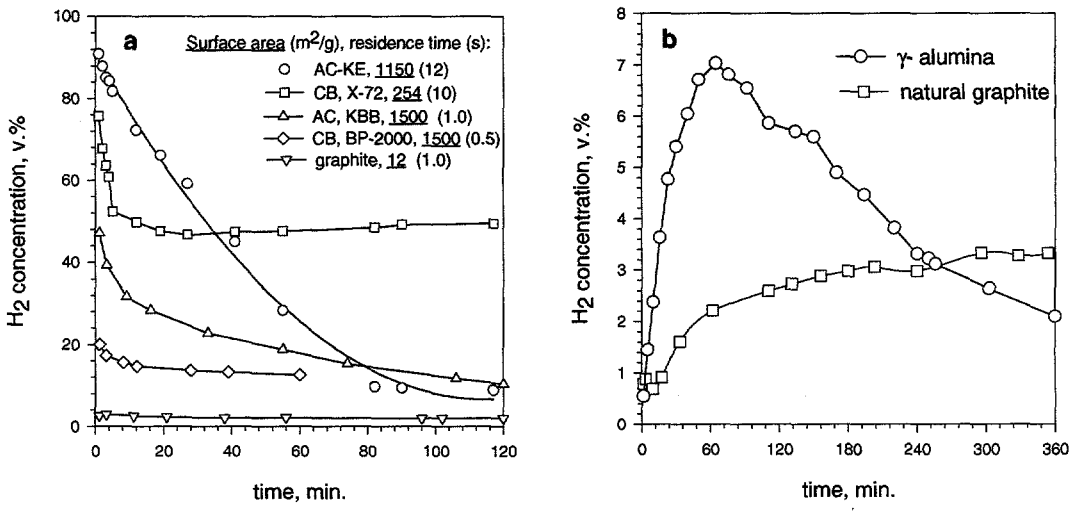

Figure 5-2. Methane Decomposition over Different Carbon Catalysts at 850°C

Over period of 6 hours the process reached quasi-state regime which lasted for 9 hours, after which the methane decomposition rate slowly declined. No methane decomposition products other than hydrogen and carbon and small amounts of C_2 hydrocarbons ($\Sigma(C_2H_4+C_2H_6)< 0.3$ v.%) were detected in the effluent gas during the entire process. The amount of carbon produced corresponded to the volume of H_2 within the experimental margin of error (5%).

Figure 5-3 (right) shows the kinetic curves of methane decomposition over different forms of carbon blacks at relatively high space velocities (or low residence times, approx. 1 s), which explains low methane decomposition yields.

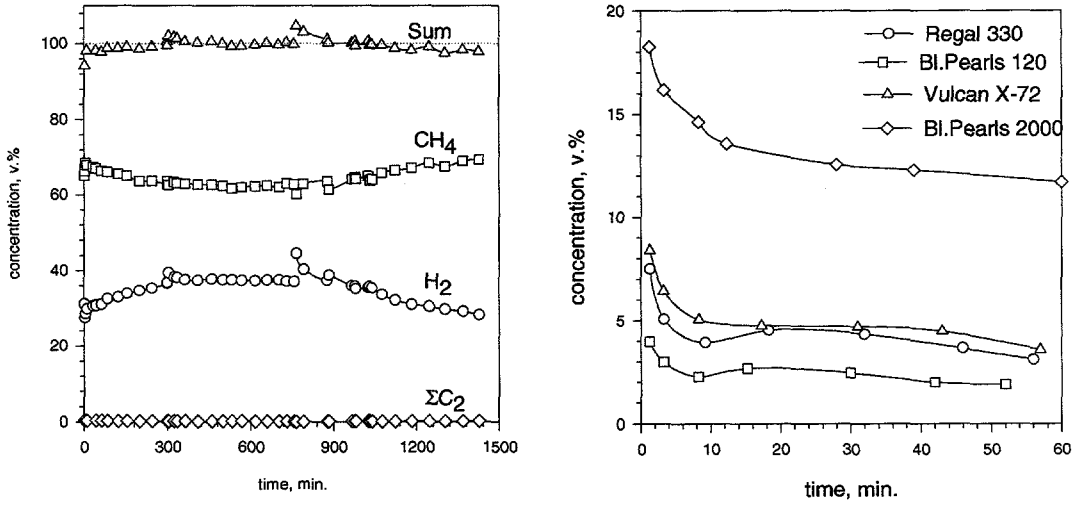

Figure 5-3. Methane Decomposition over Acetylene Black (left) and Different Carbon Blacks (right) at 850°C

Figure 5-4 demonstrates the results of methane decomposition over different samples of activated carbon at 850°C. These experiments were purposely conducted at low residence times (approx. 1 s) in order to differentiate the kinetic curves, which otherwise would be very close to each other. This resulted in some drop of hydrogen concentration in the effluent gas. However, the trend is apparent: all samples of activated carbon, regardless their origin, showed very close initial activity in methane decomposition, but rapidly deactivated over the period of one hour.

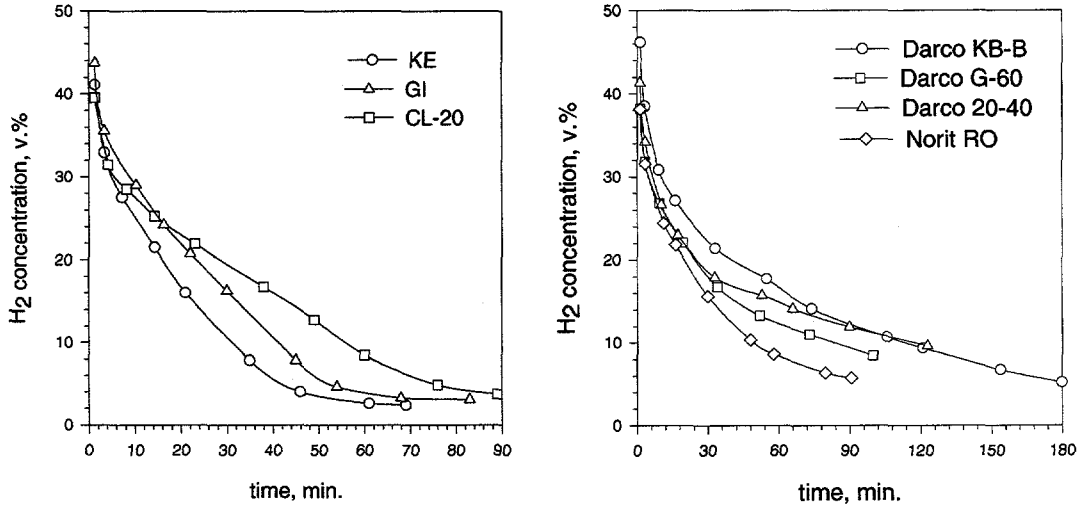

Figure 5-4. Methane Decomposition over Different Activated Carbons at 850oC

Figure 5-5 depicts the kinetic curves of methane decomposition over some "exotic" forms of carbon, including fullerenes and carbon nanotubes. It is apparent that glassy carbon and fullerenes C_{60} demonstrated relatively high initial activity, but very low stability toward methane decomposition reaction.

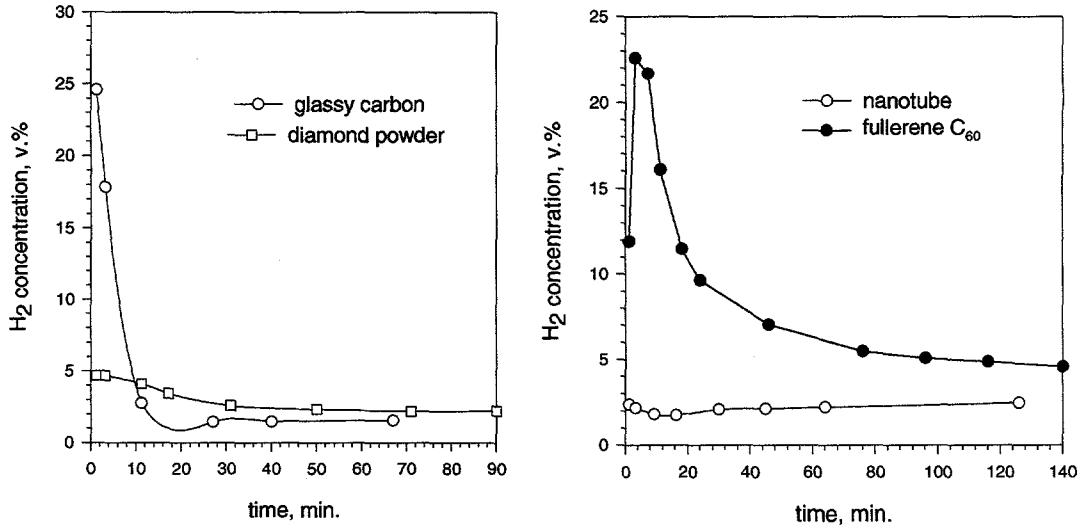

Figure 5-5. Methane Decomposition over Glassy Carbon, Diamond Powder, Fullerene C_{60} and Carbon Nanotubes

According to the Table 5-1 and Figure 5-2 graphites have the lowest initial catalytic activity (per unit of weight) in methane decomposition reaction. Among other factors, this could be attributed to the low surface area of graphites. However, the following experimental observation proves that graphites are indeed catalytically inert toward methane decomposition.

It was found that the initial methane conversion rates in the presence of synthetic and natural graphites (with SA from 3 to12 m^2/g) and three different modifications of Al_2O_3 (including α- and γ-forms) with the surface area from 6 to 275 m^2/g were in the same range of 0.2-1.0 mmol/min-g (at the same temperature and residence time). This experiment indicates that methane decomposition over graphites is most likely due to the thermal rather than catalytic processes. Inertness of graphite toward methane decomposition was earlier reported by Diefendorf [31], who demonstrated that at 800°C no methane conversion was observed over graphite surface for 2 weeks.

It is noteworthy that the sustainability factor (K_m^1/K_m^o) for natural graphite is more than unity, which indicates that the catalytic activity of carbon produced from methane is higher than that of the graphite. The same kinetic behavior was observed with both α- and γ- modifications of alumina. Figure 5-2 (b) depicts the kinetic curves of hydrogen production over natural graphite (SA=4-6 m^2/g) and γ-alumina (SA= 275 m^2/g) at 850°C and residence time of approximately 1 s. These experiments clearly point toward certain catalytic properties of carbon produced from methane. However the catalytic activity of this form of carbon is quite low and, obviously, much less than that of AC and CB-type catalysts.

These experimental results can be explained as follows. It is known that the initial rate of hydrocarbon decomposition depends on the nature of a support (substrate). As the substrate surface is covered with carbon species, the rate of methane decomposition may increase or decrease, depending on the relative catalytic activity of the substrate and the carbon produced. The total rate of the methane decomposition process is the sum of the rates of carbon nuclei formation and carbon crystallites growth. It was determined that the activation energy of the carbon nuclei formation during methane decomposition (316.8 kJ/mole) is much higher than the activation energy of the carbon crystallites growth (227.1 kJ/mole) [32]. Thus, in general, the rate of carbon crystallites growth tends to be higher than the rate of carbon nuclei production. The carbon particles produced during methane decomposition over AC catalysts, most likely, tend to have an ordered graphite-like structure and the rate of carbon crystallite growth exceeds that of nuclei formation. The catalyst surface is rapidly covered with relatively large graphite-like crystallites, which occupy active sites and result in inhibition of the catalytic activity toward methane decomposition. In the case of CB-type catalysts, the rates of crystallites growth and nuclei formation become comparable, resulting in the quasi-steady state methane decomposition. Low initial hydrogen production rate over alumina and natural graphite surface is due to high activation energy of nuclei formation over these materials. The increase in hydrogen production rate after the short induction period can be explained by the increase in the concentration of carbon nuclei on the surface and the methane decomposition rate over relatively small carbon crystallites. This is followed by the growth of the existing carbon crystallites and, as a result, the reduction of the active surface area and gradual decrease in methane decomposition rate. It case of graphite, methane decomposition rate slowly reached the steady state conversion rate controlled by the catalytic activity of carbon produced from methane. The nature of active sites responsible for the efficient decomposition of methane over the fresh surface of AC and CB catalysts is yet to be understood.

5.2. Effect of Temperature and Space Velocity on Methane Decomposition Yield

We studied the effect of temperature and methane space velocity on the yield of methane decomposition using different carbon catalysts. Figure 5-6 (a) depicts the temperature dependence of the initial H_2 concentration in the effluent gas in the presence of carbon black and activated carbon catalysts at different residence times (τ). It is clear that the initial activity of AC catalysts is higher than that of CB catalysts over the entire range of temperatures 600-1000°C.

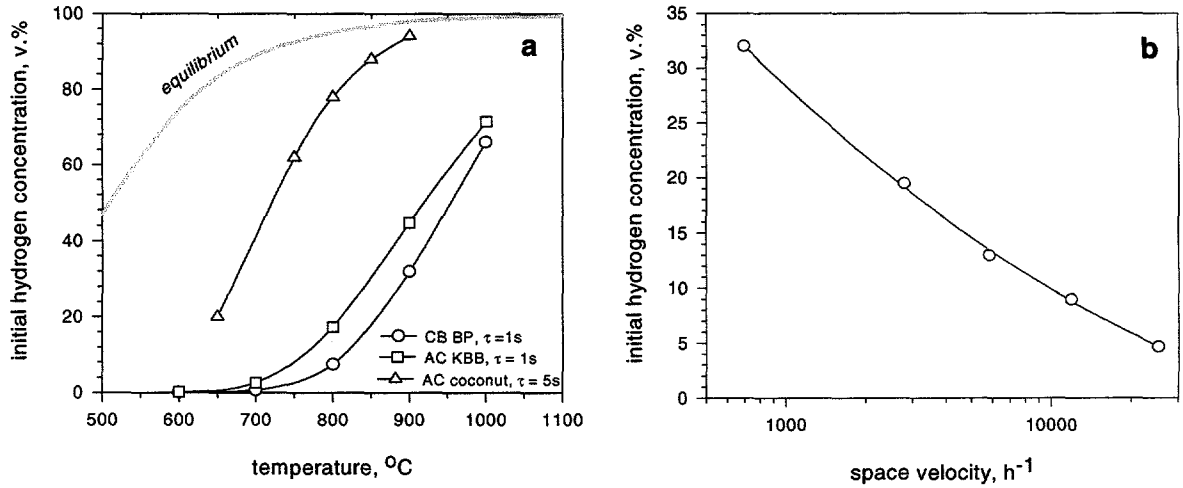

Figure 5-6. Effect of Temperature (a) and Methane Space Velocity (b) on Methane Decomposition Yield.

At sufficiently high temperatures (e.g. 900°C and higher) and residence times (e.g. 5 s and higher) the initial concentration of hydrogen in the effluent gas approaches the thermodynamic equilibrium concentration, which is an indication of high catalytic activity at these conditions. At 650°C and below the methane conversion rate was negligible.

Figure 5-6 (b) demonstrates the effect of methane space velocity on the initial concentration of hydrogen in the effluent gas produced by methane decomposition over carbon black (BP-2000) at 850°C presented in semi-log coordinates. Ten fold increase in space velocity of methane results in 3-4 fold decrease in methane decomposition yield. It should be noted that in this paper, for the sake of comparability, both the residence time and the space velocity relate to the volume of the carbon catalyst within the reactor.

5-3. Kinetic Model and Major Kinetic Parameters of CH_4 Decomposition

We developed a kinetic model of the methane decomposition reaction over carbon catalysts. It was assumed that CH_4 decomposition over the surface of carbon catalyst is controlled by two simultaneous processes:

1. decrease in methane decomposition rate due to the blocking of catalytic active sites by the carbon species produced via methane decomposition:

$$-\frac{d[CH_4]}{dt} = k_1 S_1 (1-\theta)[CH_4]$$

where, k_1- rate constant, S_1- catalyst surface area, θ- the fraction of catalyst surface covered by carbon produced from methane; θ is a function of time

2. increase in methane decomposition rate due to the formation of catalytically active carbon species produced from methane

The sum of two components results in the following kinetic equation for the methane conversion:

$$\chi_{CH_4} = e^{-k_1 S_1 (1-\theta)t} + \frac{[CH_4]_e}{[CH_4]_o}(1 - e^{-k_2 S_2 t})$$

where, χ_{CH4} is methane conversion, $[CH_4]_o$ and $[CH_4]_e$ are the initial and quasi-steady state methane concentrations in the effluent gas, respectively, S_2 and k_2, are catalyst surface area and rate constant, respectively, for methane decomposition over carbon particles produced from methane; S_2 is a function of time

The first component of the equation describes the decrease in methane conversion by the exponential decay law, whereas, the second component represents exponential rise to maximum, i.e. to the quasi-steady state value of methane conversion.

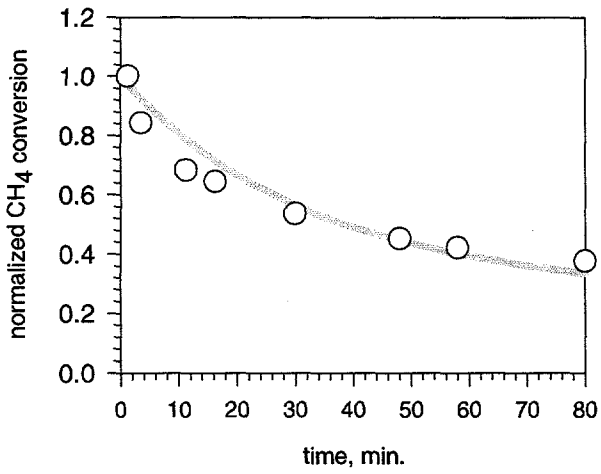

The kinetic equation obtained satisfactorily describes the experimental data during the initial stage of the methane decomposition process (1-1.5 hour). For example, Figure 5-7 compares the experimental results for methane decomposition over carbon black (BP-2000) catalyst at 850°C (circles) with the curve produced by fitting the data to the above kinetic model (gray line). The model can explain the peculiarities of the kinetic curves for methane decomposition over different types of carbon catalysts.

Figure 5-7. Experimental Data (circles) and Curve Fit Using Kinetic Model (gray line)

The initial catalytic activity of AC is much higher than that of carbon produced from methane, therefore, the second component of the kinetic equation could be neglected, which results in a typical exponential drop shape of the kinetic curve. In contrast to AC, graphite catalysts (particularly, natural graphite) have very low initial catalytic activity toward methane

decomposition reaction, therefore the first component of the kinetic equation is negligible, and the resulting kinetic curve is either flat, or is described by the exponential rise to maximum law (see also Figure 5-2, b). The same is true for the methane decomposition over alumina surface.

We determined the kinetic parameters of methane decomposition reaction over different carbon catalysts. Table 5-2 summarizes the major kinetic parameters (apparent reaction rate constants, frequency factors and activation energies) for CB and AC catalysts at the range of temperatures 700-900°C.

Table 5-2. Apparent Reaction Rate Constants and Activation Energies for CH_4 Decomposition over CB and AC Catalysts

Catalyst	T°C	k, s^{-1}	E_a, kJ/mol	α, s^{-1}
Carbon black, BP-2000 SA= 1500 m^2/g	750	0.035	235.9	4.3×10^9
	850	0.480		
	950	2.125		
Activated carbon, KBB SA= 1500 m^2/g	600	0.0015	200.7	4.9×10^8
	700	0.026		
	800	0.178		
	900	0.602		

Thus, the apparent rate constants for methane decomposition in the presence of carbon black BP-2000 (k_{CB}) and activated carbon KBB (k_{AC}) catalysts could be expressed as follows:

$k_{CB} = 4.3\times10^9 \exp(-235.9/RT)$ 750-950°C

$k_{AC} = 4.9\times10^8 \exp(-200.7/RT)$ 600-900°C

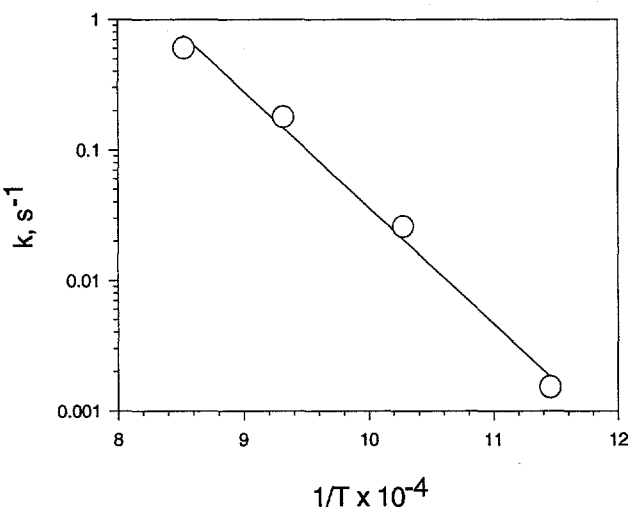

Figure 5-8 depicts the Arrhenius plot for methane decomposition over AC (KBB) catalyst. The activation energies of methane decomposition reactions over carbon catalysts are characteristic of surface reaction rate controlled processes.

Figure 5-8. Arrhenius Plot for CH_4 Decomposition

5.4. Catalytic Pyrolysis of Propane over Carbon Catalysts

Due to a relatively weak C – H bond in propane molecule (402.2 kJ/mol) it is somewhat easier to split propane than methane molecule (methane C – H bond energy is 440.0 kJ/mol). 26.0 kJ is required to produce one mole H_2 from propane, comparing that to 37.8 kJ for methane:

$$C_3H_8 \rightarrow 3C + 4H_2 \qquad \Delta H^o = 103.9 \text{ kJ/mol}$$

However thermal cracking of propane at high temperatures proceeds via a thermodynamically more favorable formation of methane and ethylene:

$$C_3H_8 \rightarrow CH_4 + C_2H_4 \qquad \Delta H^o = 81.3 \text{ kJ/mol}$$

Therefore, during pyrolysis of propane, in most cases, we observed the production of gaseous mixture containing hydrogen, methane, ethylene and small amounts of ethane and propylene. Figure 5-9 depicts the experimental results of propane catalytic pyrolysis over CB (a) and AC (b) type catalysts at 800°C in a packed bed reactor. Similar to methane decomposition, activated carbon demonstrated high initial activity followed by the rapid drop in catalytic activity. At the onset of the process hydrogen and methane were the only products of propane pyrolysis. Practically no C_2^+ byproducts were found in the effluent gas during first 10 min.

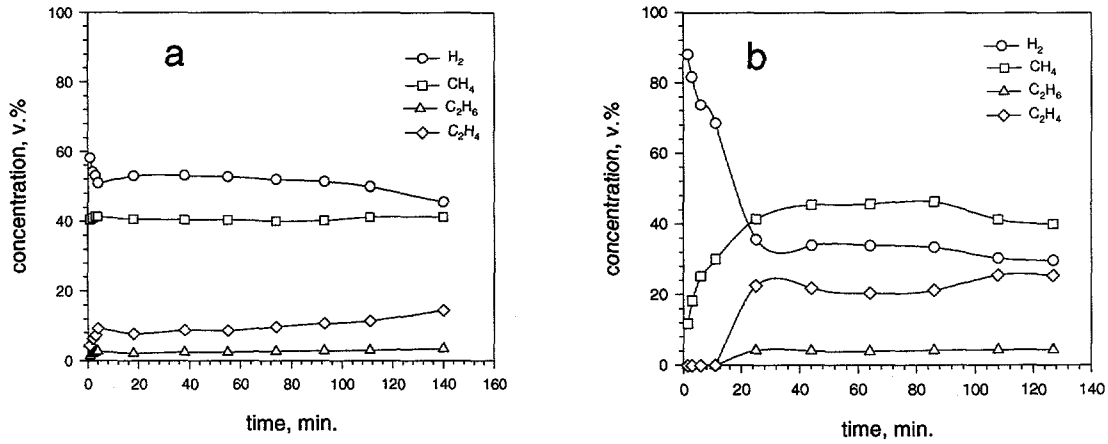

Figure 5-9. Propane Pyrolysis over CB (XC-72) (a) and AC (KE) (b) at 800°C

Quasi-steady state pyrolysis of propane was established after 30-40 min with methane being the major product of pyrolysis and significant concentration of ethylene in the effluent gas.

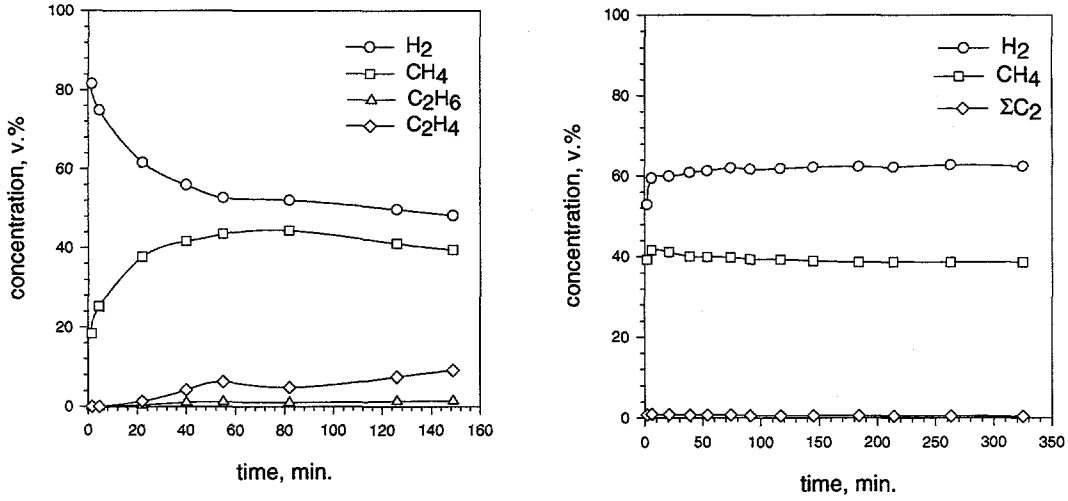

Figure 5-10. Propane Pyrolysis over Activated Carbon (Phenol Resin) (800°C) (left) and Acetylene Black (850°C) (right)

The composition of the effluent gas of propane pyrolysis over AC catalyst approximately corresponded to the following chemical equation:

$$C_3H_8 \rightarrow 0.8\ H_2 + CH_4 + 0.6C_2H_4 + 0.8C \qquad \Delta H^o = 60.3\ kJ/mol$$

Propane pyrolysis over carbon black was characterized by lower initial rate, but was more sustainable comparing to AC catalyst, as shown on Figure 5-9 (a). Quasi-steady state rate of propane pyrolysis was reached in approximately 5 min and the process remained stable for approximately 2 hours. Hydrogen was a major component of the effluent gas during CB-catalyzed pyrolysis of propane.

Figure 5-10 depicts the results of propane pyrolysis over activated carbon produced from phenol resin (left) and acetylene black (right). As in previous cases, AC-type catalyst demonstrates higher initial activity and lower stability, comparing to CB-type catalysts.

5.5. Catalytic Pyrolysis of Liquid Hydrocarbons

From the thermodynamic point of view the decomposition (pyrolysis) of liquid hydrocarbons is more favorable than the decomposition of methane, as almost 1.5-2 times less energy is required to produce a unit volume of hydrogen. We conducted a series of experiments on the catalytic pyrolysis of a wide range of liquid hydrocarbons (hexane, octane, gasoline and diesel fuel) using different carbon-based catalysts.

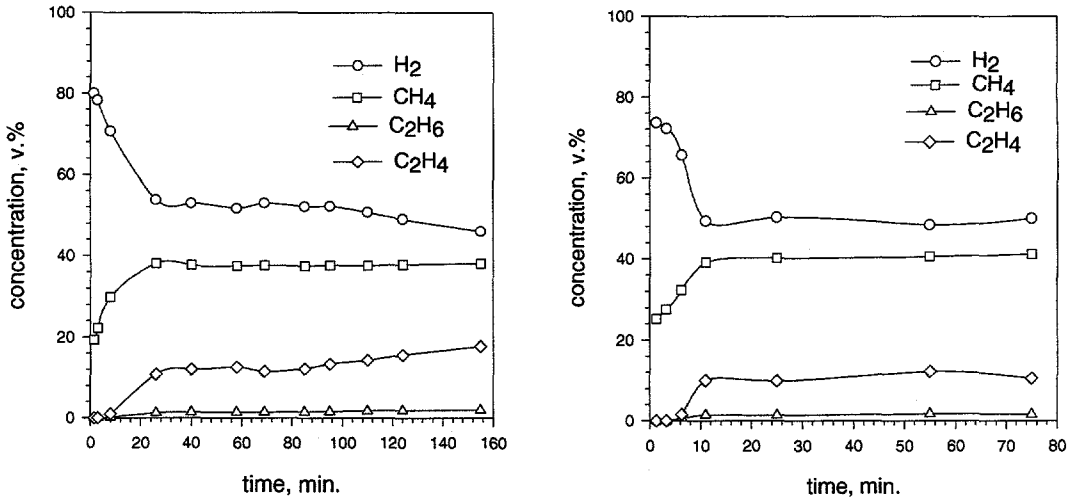

Figure 5-11. Pyrolysis of Hexane (left) and Gasoline (right) over Activated Carbon (Phenol Resin) at 800°C Gasoline

Figure 5-11 depicts the experimental results of the catalytic pyrolysis of hexane and gasoline over carbon catalysts at 800°C. In both cases, the quasi-steady state production of the pyrolysis products was achieved over period of 10-20 min. After 1-1.5 hours we observed the production of small amounts of the dark liquid products. The gas production rate reached 700 mL/min per mL/min of gasoline. In the case of diesel fuel the concentration of hydrogen in the effluent gas with one reactor arrangement was in average 30-40%v.

5.6. Characterization of Carbon Catalysts

5.6.1. XRD Studies of Carbon Catalysts

We conducted X-ray Diffraction (XRD) studies of the original carbon catalysts and carbon samples produced during hydrocarbon (methane or propane) decomposition. Figure 5-12 depicts the sample holder geometry.

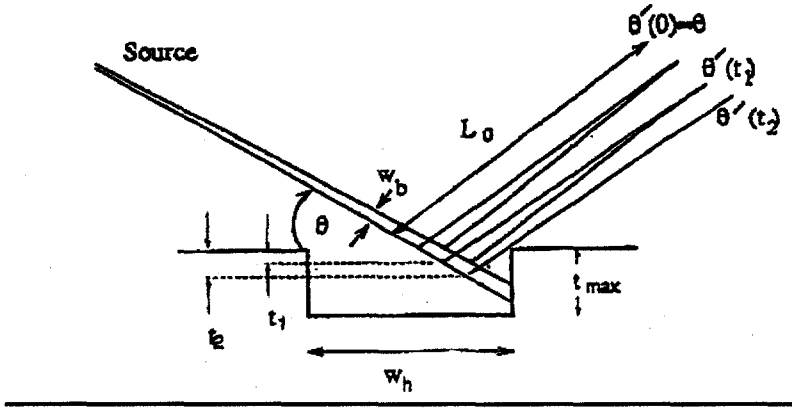

Figure 5-12. XRD Sample Holder Geometry

On this Figure t_{max} is sample holder depth, w_h- holder width, w_b- beam width, L_o-goniometer radius. Typical parameters for the diffraction scans are detailed below.

- D/MAX 2200T/PC ULTIMA+ Theta/Theta Goniometer, 185 mm radius, 6° take-off angle
- Configuration for standard diffraction for phase identification:
- continuously variable divergence slit (computer controlled)
- continuously variable anti-scatter slit
- 0.30 mm receiving slit
- 0.8 mm monochromator receiving slit
- curved crystal graphite monochromator
- scintillation counter
- source: Cu anode X-ray tube
- generator settings: 50kV/40 mA

Carbon black BP-2000 with the surface area of 1500 m^2/g and activated carbon Darco KBB (produced from hardwood) with the same surface area were used in these studies. Figure 5-13 depicts XRD spectrum of the original carbon black (BP-2000) sample used in the experiments. Figure 5-14 demonstrates XRD spectrum of the carbon sample produced by propane pyrolysis at 850°C. It was found that the original sample had one- or, possibly, some two-dimensional ordering, whereas, sample produced from propane had ordering in the "columnar" or stacking (003) direction. The following diagram illustrates this concept:

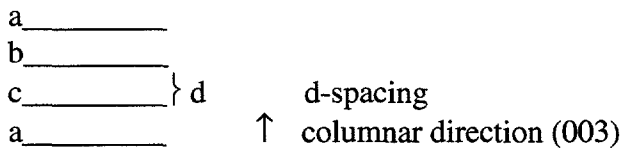

where, a, b, and c are alternating arrangements of carbon ring plates. The d-spacing (lattice spacing) or spacing between plates is practically uniform, so that the (003) columnar reflection is clearly present. Thus, carbon produced during propane pyrolysis clearly has a typical graphite a-b-c-a type stacking of the carbon ring plates.

The actual d-spacing (d =3.4948 Å) of this (003) peak is larger than that of the standard graphite structure (d = 3.3480 Å), which indicates that the plates are slightly further apart in the columnar stacking direction. This reflection is almost absent in the original carbon black sample which indicates that the plates are not stacked in a columnar arrangement, but, instead, are randomly oriented with respect to each other. The other two crystalline diffraction peaks in carbon sample produced by propane decomposition (43.5 and 46.2°2θ) also result from the three dimensional ordering, and result from the regular arrangement of spacings in various directions with respect to the columnar direction. The peaks 62.2 and 67. 2°2θ are due to scattering rather than to crystalline diffraction. The peak at 62.2 is due to C – C atomic distance for atoms which are out-of-plane, and the peak at 67.2 results from the C – C atomic distance for the in-plane carbon atoms.

The size of graphite crystallite produced by propane decomposition was estimated at 23 Angstrom (Figure 5-15). The following is a profile fitting results:

2-Theta	25.549 (0.018)
d(A)	3.4836 (0.0047)
Height	2150 (11)
Area	277158 (1727)
Shape	0.870
Skew	0.491
FWHM Breadth	5.156
XS(A)	23 (1)

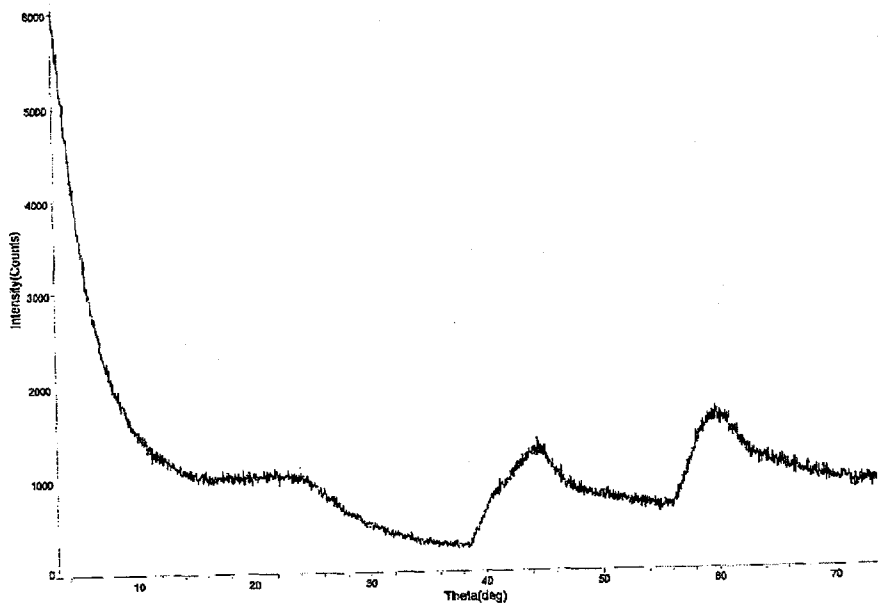

Figure 5-13. XRD Spectrum of Carbon Black BP-2000

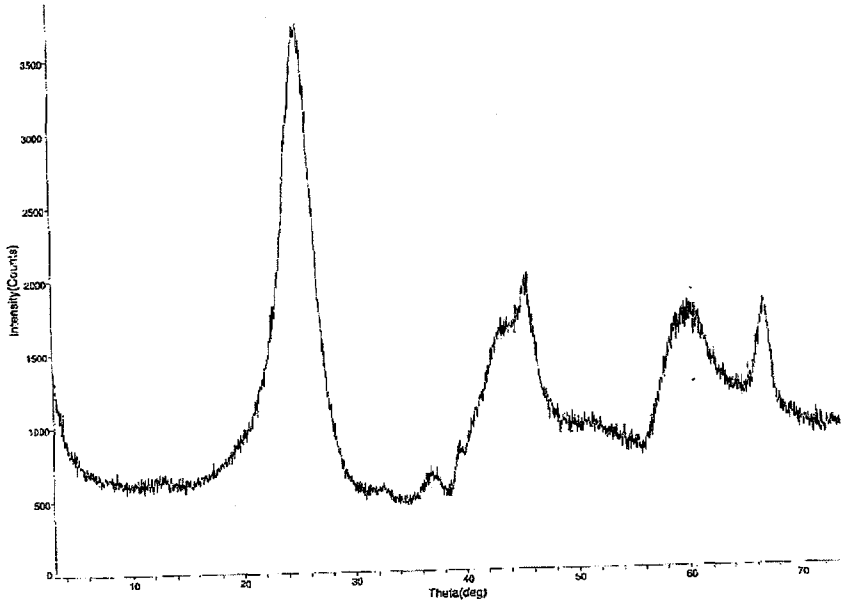

Figure 5-14. XRD Spectrum of Carbon Produced by Propane Pyrolysis over Alumina

Figures 5-16 and 5-17 show XRD spectra of carbon samples produced by decomposition of ethylene over carbon black BP-2000.

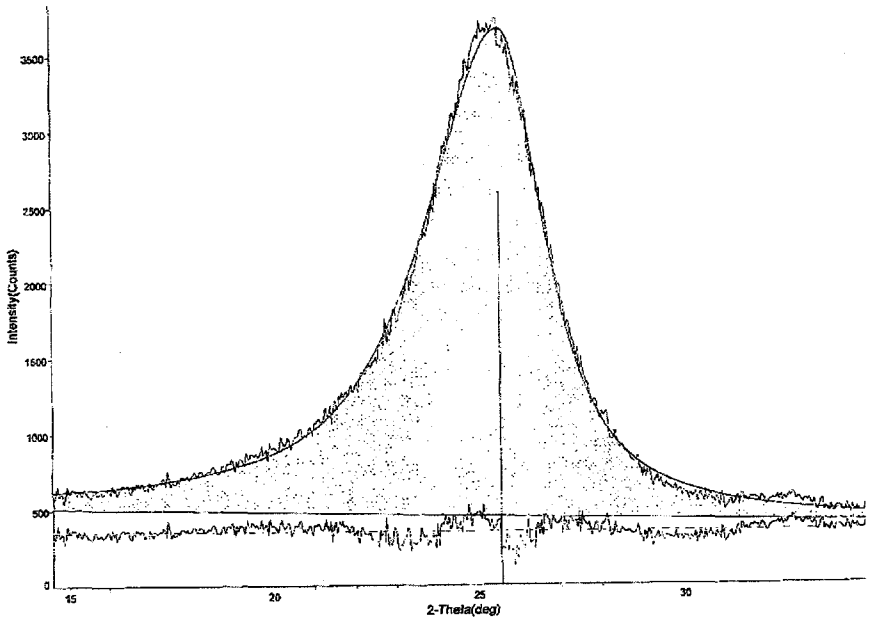

Figure 5-15. XRD Spectrum Profile Fitting for Carbon Produced by Propane Pyrolysis

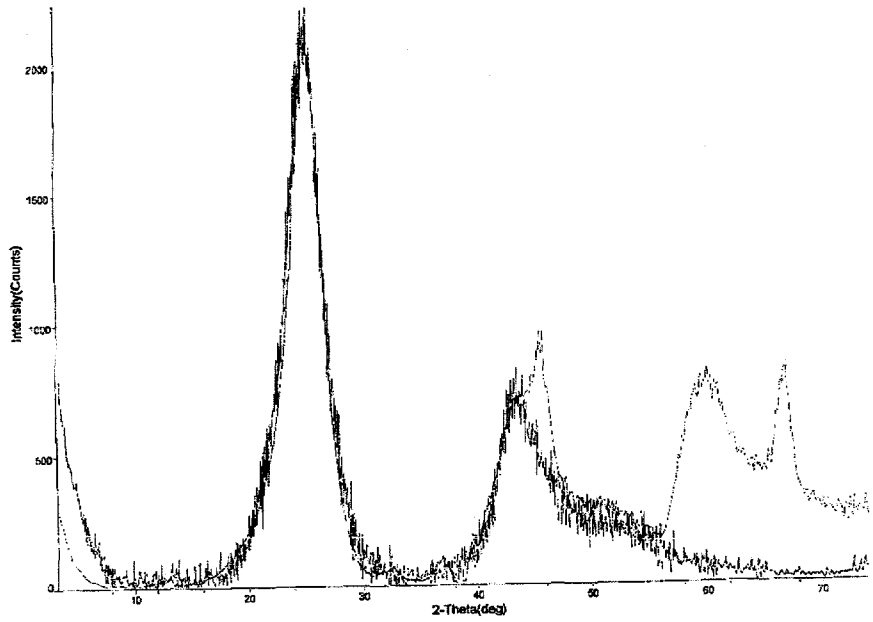

Figure 5-16. XRD Spectrum of Carbon Produced by Ethylene Pyrolysis over Carbon Black (BP-2000)

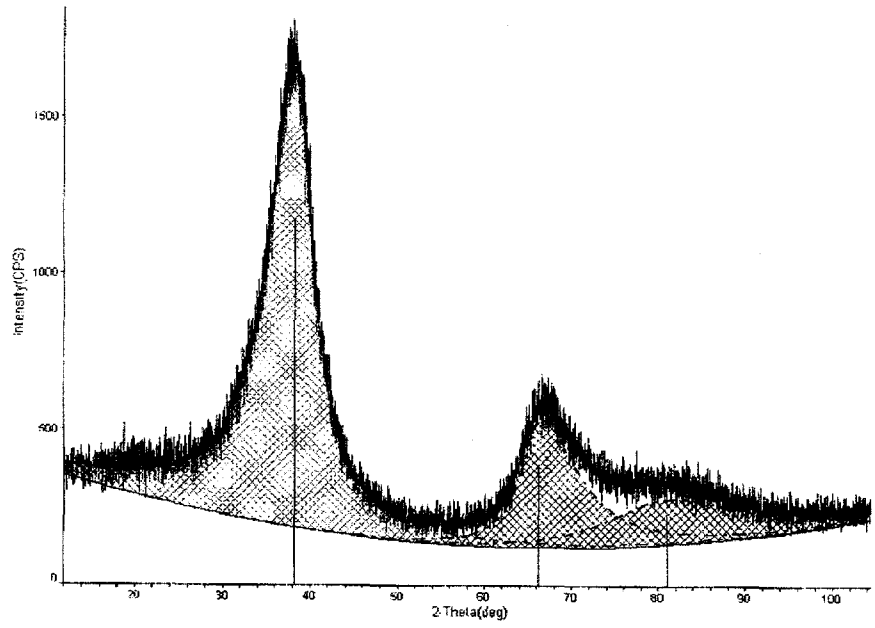

Figure 5-17. XRD Spectrum Profile Fitting for Carbon Produced by Ethylene Pyrolysis

XRD spectrum of the sample of activated carbon (Darco KBB) also indicated the lack of clear three dimensional ordering. Thus, XRD studies confirmed that carbon species produced by decomposition of alkanes (methane and propane) at 850°C predominantly have an ordered (graphite-like) structure. This fact explains the gradual drop in the activity of AC and other carbon catalysts during methane and propane pyrolysis.

5.6.2. SEM Studies of Carbon Catalysts

We conducted Scanning Electron Microscope (SEM) studies of the surface of carbon catalysts. Average particle size of powdered activated carbons was 40-100 μm. Carbon black particles were significantly smaller in size and varied in the range of 0.1 – 1 μm. Figure 5-18 depicts SEM micrographs of CB (BP-2000) catalyst before exposure to hydrocarbons at different magnifications.

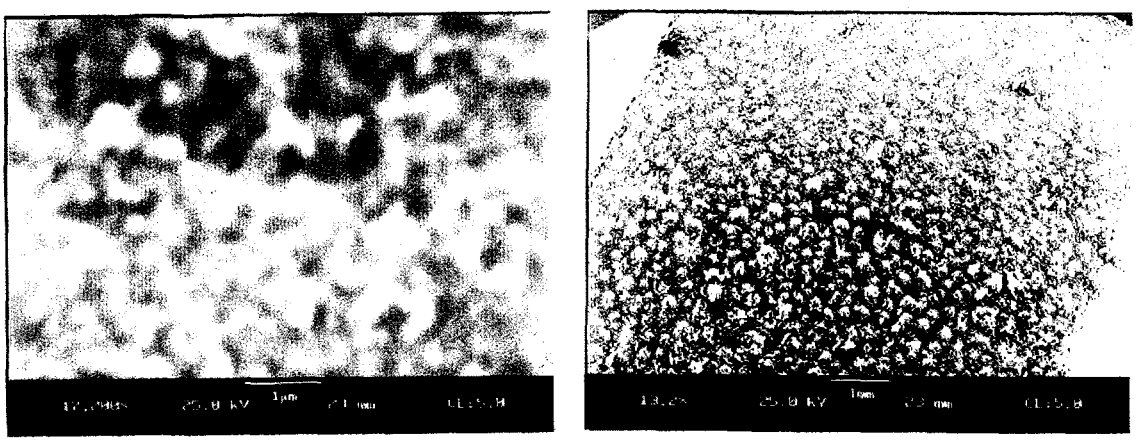

Figure 5-18. SEM Micrograph of Carbon Black (BP-2000)

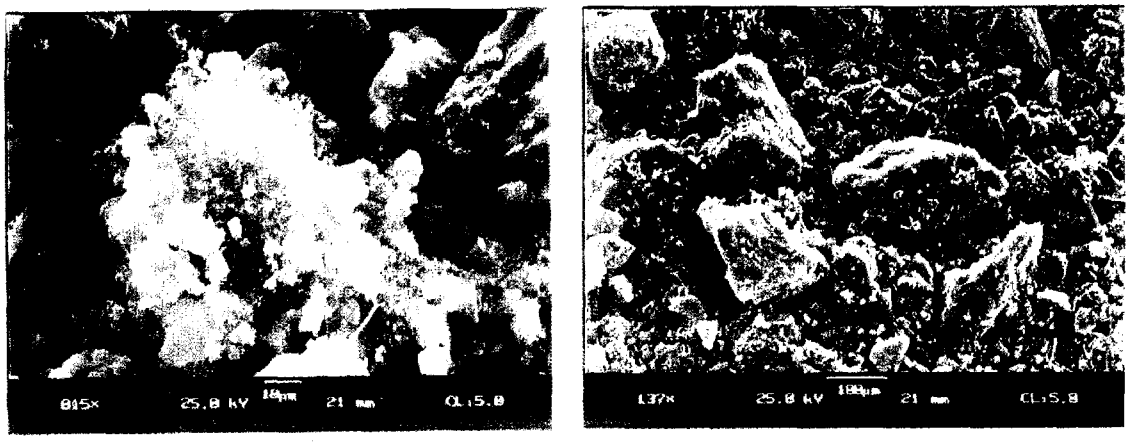

Figure 5-19. SEM Micrograph of Carbon Produced by Decomposition of CH_4/C_3H_8 Mixture over Carbon Black (BP-2000)

Figures 5-19 and 5-20 demonstrate SEM micrographs of carbon produced by decomposition of CH_4/C_3H_8 gaseous mixture and propane, respectively, over the surface of carbon black BP-2000. It is obvious that CH_4/C_3H_8 mixture produces carbon sample with less uniform distribution of carbon crystallites comparing to propane.

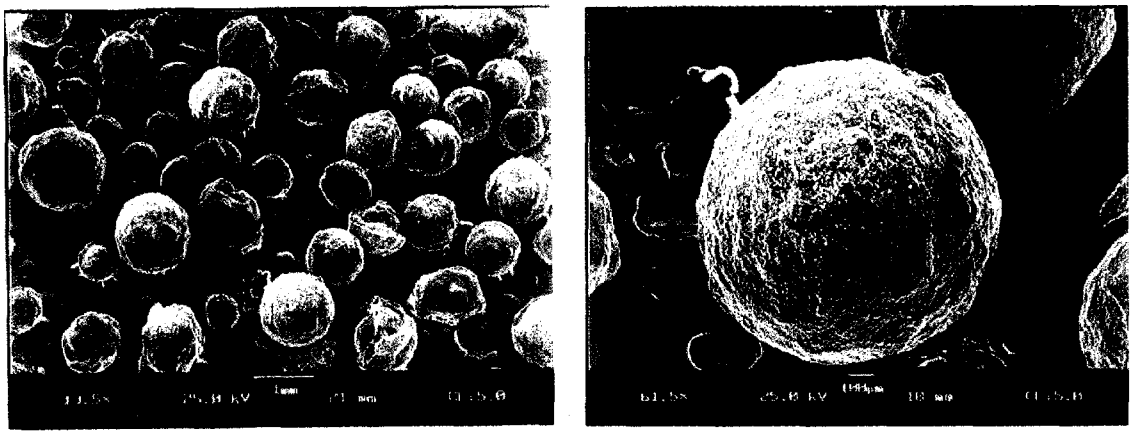

Figure 5-20. SEM Micrograph of Carbon Produced by Decomposition of C_3H_8 over Carbon Black (BP-2000)

It can be seen that in case of propane the average diameter of carbon particles increased from 0.1-0.3 μm (for the original carbon sample) to approximately 0.1-1 mm due to carbon deposition during propane pyrolysis, which corresponded to more than thousand fold increase in particles mean diameter. On the other hand, the amount (weight) of carbon in the reactor increased only 6

times as a result of propane pyrolysis. This implies that a great deal of the agglomeration of carbon particles occurred during the process. Surface area calculations indicate that propane pyrolysis over CB catalyst would result in the reduction of the total geometrical surface of carbon particles by two orders of magnitude. This would have led to a drastic decrease in propane pyrolysis rate due to a significant reduction in the catalytic surface, which did not happen. The reason for that is that the actual surface area of each particle was much higher than its geometrical surface due to the presence of clusters of carbon particles about 3-10 μm in diameter on the surface of the larger carbon particles (not shown on the micrograph).

5.6.3. Carbon Particle Size and Distribution Measurements

Carbon particle sizing was performed using ACCUSIZER 770/SPOS Single Particle Optical Sizer. The ACCUSIZER 770 uses the method of single-particle optical sensing (SPOS) to quickly count and size a large number of particles, one at a time, thus constructing the true particle size distribution (PSD). The ACCUSIZER uses autodilution, which automatically dilutes the starting sample to the optimum concentration. SPOS is a measurement based on the population of particles. Figures 5-21 through 5-23 show the results of carbon particle size and distribution using acetylene black and graphite samples. For example, Figure 5-21 demonstrates that mean particle size for acetylene black sample was 0.77 μm (measured by SPOS method). The total number of particles in the sample was 1099992, dilution: 5.52. The carbon particle size measured by Dynamic light scattering method (DLS) was in the range of 330-470 nm (or 0.33-0.47 μm). This does not agree with the size of acetylene black particles (0.042 μm) reported in the product specification, which indicates that the carbon particle aggregation most likely occurred during sample preparation and particle size measurements.

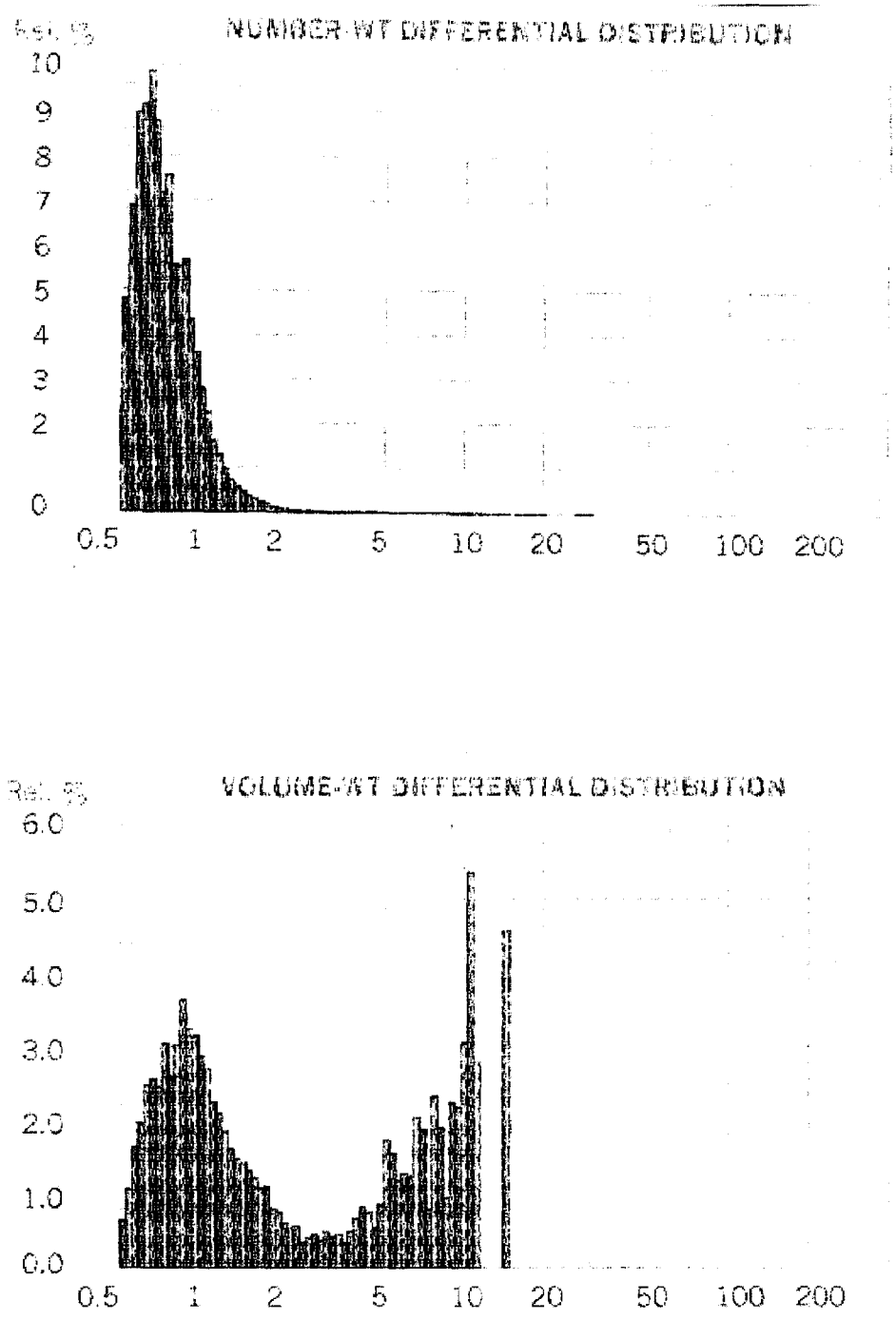

Figure 5-21. Acetylene Black Particle Size Measurements Using Model 770 Accusizer

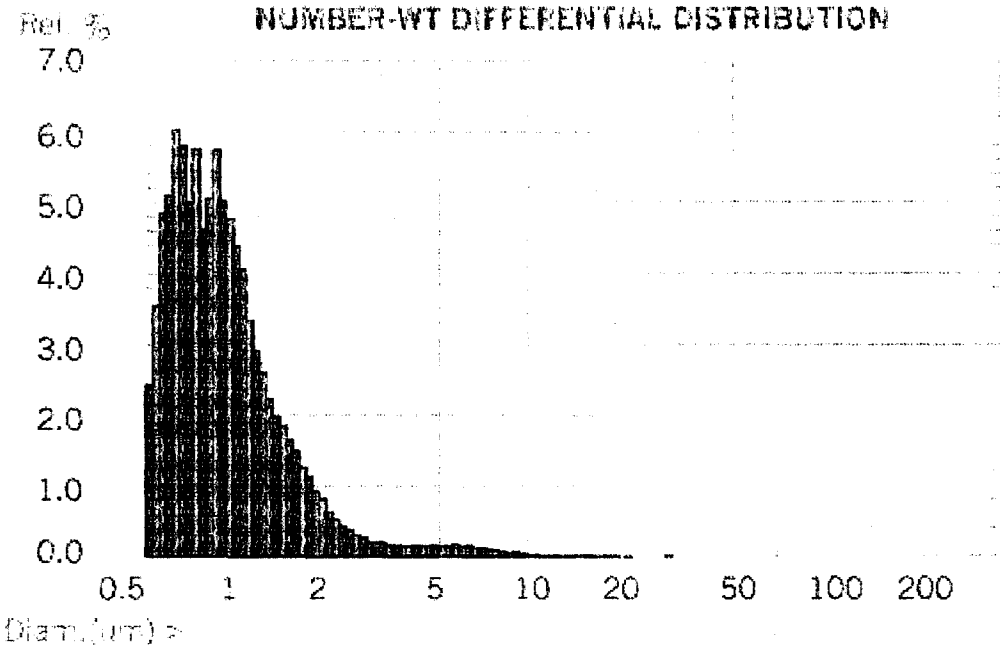

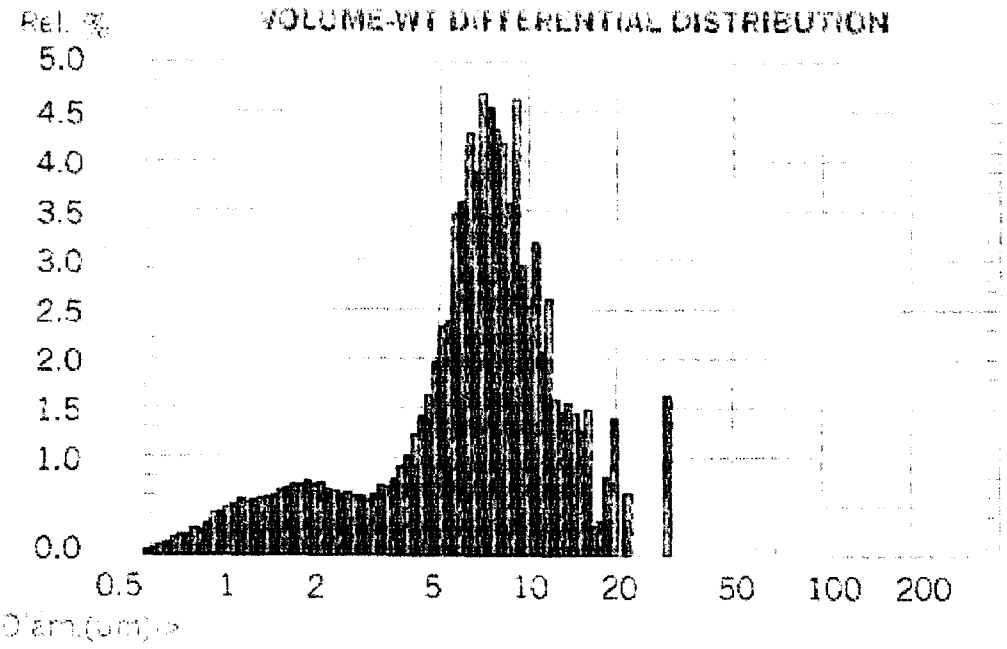

Figure 5-22. Graphite Particle Size Measurements Using Model 770 Accusizer

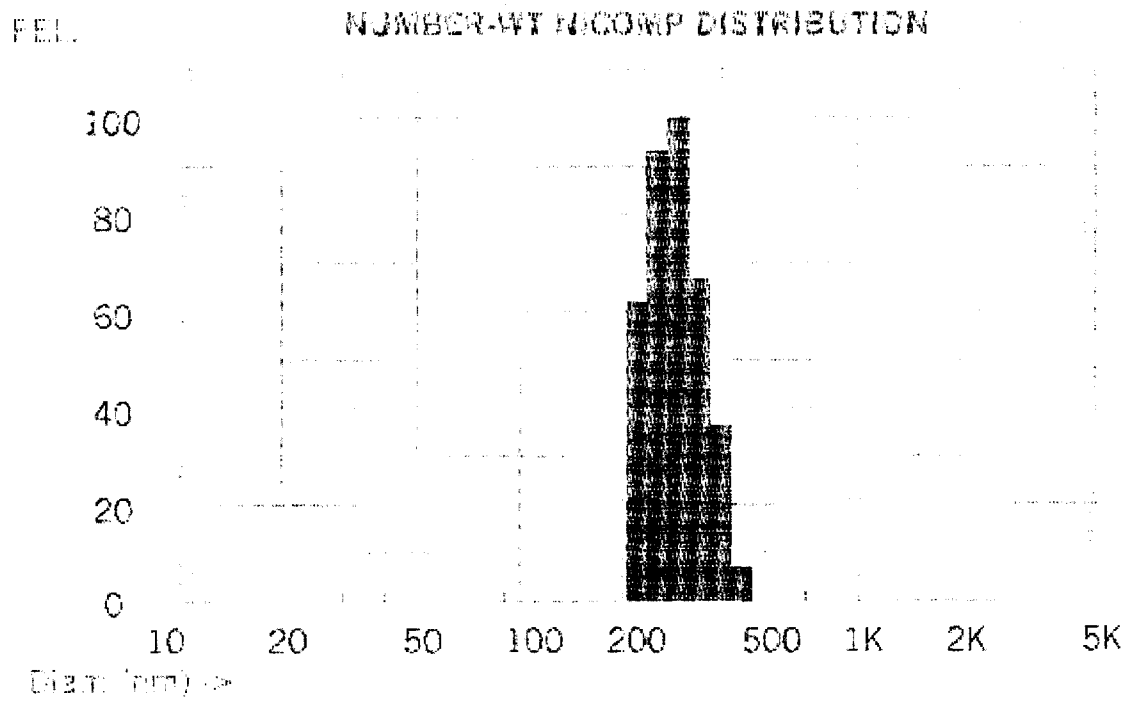

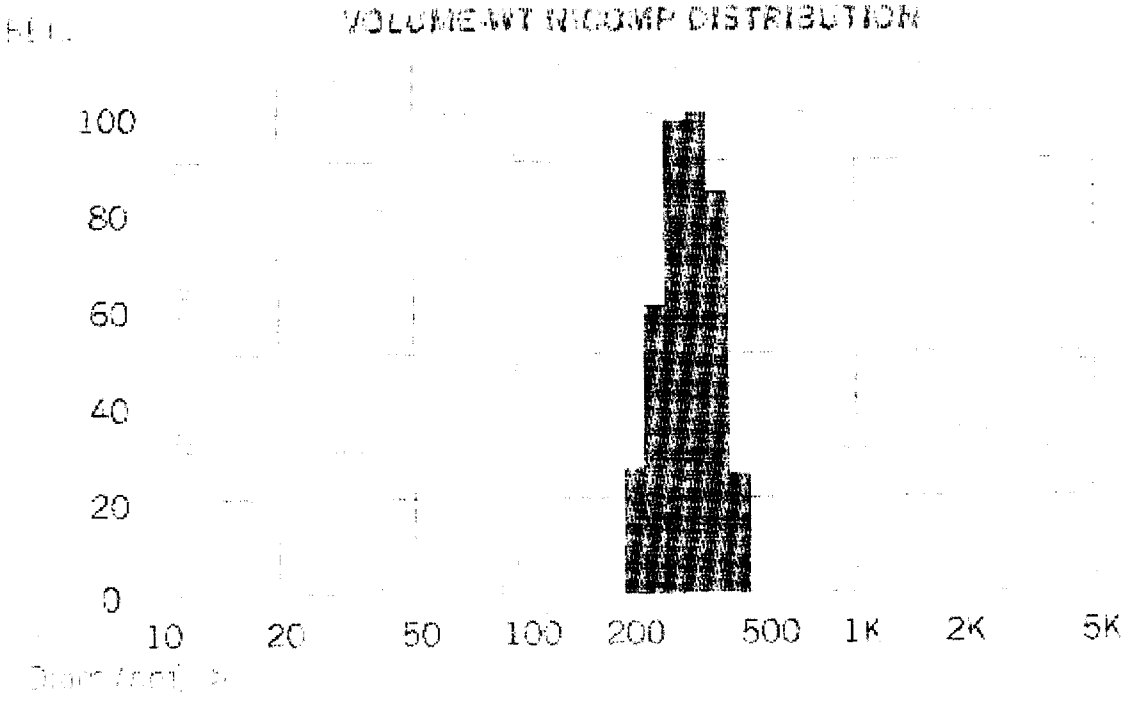

Figure 5-23. Acetylene Black Particle Size Measurements

For the graphite sample, mean particle size was estimated at 1.09 μm (number-weight) and 7.76 μm (volume weight), which is in a good agreement with the data provided by the manufacturer on the graphite particle size (2-15 μm).

5.7. Thermocatalytic Reactors for Hydrocarbon Decomposition

The objective was to conduct studies on various conceptual designs for the thermocatalytic reactor for hydrocarbon decomposition. The reactors were designed, fabricated and tested for the simultaneous production of hydrogen and carbon using methane, propane and gasoline as feedstocks.

5 different types of reactors for hydrocarbon decomposition were considered:

- packed bed reactor (PBR)
- tubular reactor (TR)
- free volume reactor (FVR)
- fluid wall reactor (FWR)
- fluidized bed reactor (FBR)

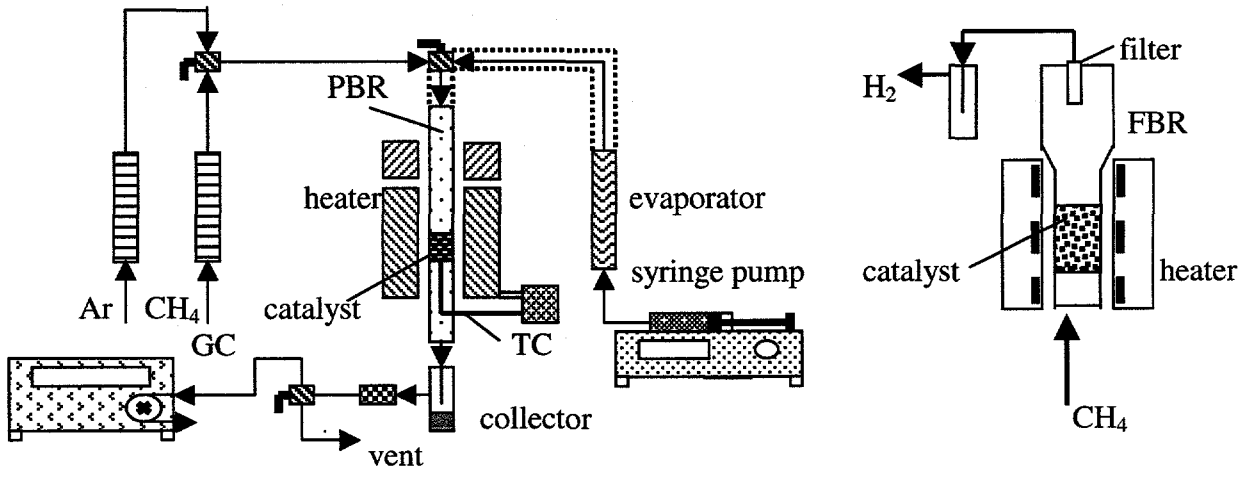

GC- gas chromatograph, TC- thermocouple

Figure 5-24. Schematic Diagram of the Experimental Set-up with PBR (left) and FBR (right) Reactors

Figure 5-24 demonstrates the experimental set-up with a packed bed reactor (left) used for the decomposition of methane, propane and gasoline. It should be noted that the same experimental set-up was also used for testing of the fluidized bed (right) and other reactors.

5.7.1. Packed Bed Reactor

PBR was mainly used for carbon catalysts screening, and studies on the effect of operational parameters (temperature, space velocity) on hydrogen yield, and kinetic measurements. Several examples of PBR test runs are presented in the Table 5-3. In some cases, it was difficult to conduct long run experiments with PBR due to carbon build up within the reactor and potential reactor clogging. It is apparent that the continuous removal of carbon from PBR would be a daunting technical problem, therefore, this type of the reactor is unlikely to be used in large scale hydrogen production units.

5.7.2. Tubular Reactor

We have conducted a series of experiments on fast pyrolysis of methane using ceramic (alumina) and quartz tubular reactors. The objective was to thermally (homogeneously) decompose methane to hydrogen, carbon and valuable unsaturated and aromatic hydrocarbons. Preliminary testing of the catalytic activity of quartz and alumina toward methane decomposition reaction proved their inertness at temperatures below 1100°C. The tubular reactors with the internal diameters of 3-6 mm and a small reaction zone enabling to achieve the residence times in the range of 1-20 milliseconds, were used in these experiments. Preheated (400°C) methane streams entered the reactor at flow rates in the range of 1-10 l/min and were subjected to pyrolysis at the temperatures of 900-1100°C. The conversion of methane was found to be a function of the temperature and residence time. For example, at the reaction zone temperature of 1100°C and residence times of 1.0, 2.0 and 6.2 ms, methane conversions were 0.1, 2.0 and 16.1%, respectively. Hydrogen and carbon were the main products of pyrolysis accounting for more than 80 w.% of the products. Unsaturated (mostly, C_2) and aromatic (including polynuclear) hydrocarbons were also produced in significant quantities as byproducts of methane pyrolysis. For example, at the reaction zone temperature of 1100°C and the residence time of 6.2 ms the yields of gaseous and liquid products were as follows (mol.%): C_2H_6- 0.9, C_2H_4- 3.3, C_2H_2- 5.8, C_2-C_6- 1.5, polynuclear aromatics (naphthalene, anthracene)- 2.0. Unidentified liquid products of pyrolysis accounted for approximately 5 w.% of methane pyrolysis products. Carbon (coke) was mostly deposited on the reactor wall down-stream of the reaction zone, which indicated that methane decomposition reaction occurred predominantly homogeneously in gas phase. At higher residence times (seconds and minutes scale), the yields of C_2^+ and polyaromatic hydrocarbons dramatically dropped. These experiments demonstrated that methane decomposition process could be arranged in a homogeneous mode producing not only hydrogen and carbon, but also a variety of very valuable hydrocarbons (ethylene, acetylene, aromatics).

The mechanism of thermal decomposition (pyrolysis) of methane has been extensively studied [33]. Since C - H bonds in methane molecule are significantly stronger than C - H and C - C bonds of the products, secondary and tertiary reactions contribute at the very early stages of the reaction, which obscure the initial processes. It has been shown [33] that the homogeneous dissociation of methane is the only primary source of free radicals and controls the rate of the overall process:

$$CH_4 \rightarrow CH_3^{\cdot} + H^{\cdot}$$

This reaction is followed by a series of consecutive and parallel reactions with much lower activation energies. After the formation of acetylene (C_2H_2), a sequence of very fast reactions occurs leading to the production of higher unsaturated and aromatic hydrocarbons and finally carbon:

C_2H_2 → high unsaturated hydrocarbons → aromatics → polynuclear aromatics → carbon

This involves simultaneous decomposition and polymerization processes and phase changes from gas to liquid to solid. A detailed mechanism of the final transformations to carbon is rather complex and is not well understood.

These experiments demonstrated that TR could potentially be scaled up for the use in full scale methane decomposition process, although, it would require the elevated temperatures (above 1000°C) and special surface-treated tubes to prevent carbon deposition in the reaction zone.

5.7.3. Free Volume Reactor

Free volume reactor is designed to carry out high temperature reactions by contacting a reagent gas with a stream of preheated carrier gas. FVR could be advantageous for the conducting of different dissociation reactions with formation of solid phase products, including methane decomposition reaction. In our work we designed and tested FVR for a continuous production of hydrogen and carbon via methane decomposition. Methane decomposition occurred homogeneously by contacting a hot carrier gas such that carbon was produced in a free volume of the reactor and carried away by the gaseous stream, thus preventing carbon from deposition on the reactor wall. Two options for introducing thermal energy into the reaction zone were considered: by the stream of inert gas (Ar) or hydrogen. Figure 5-25 shows the schematic diagram of FVR used for decomposition of methane and propane. Methane was introduced into the reactor through the inner ceramic tube, and the heat carrier gas entered the space between the inner and outer (quartz) tubes of FVR. We used Ar or hydrogen as heat carrier gases in a ratio 4:1 (by volume) to methane. The heat carrier gas was heated by the electric heater to 1200-1300°C and entered the reaction zone where it contacted the preheated stream of methane. The results of the FWR testing using hydrogen as a carrier gas are presented in the Table 5-3.

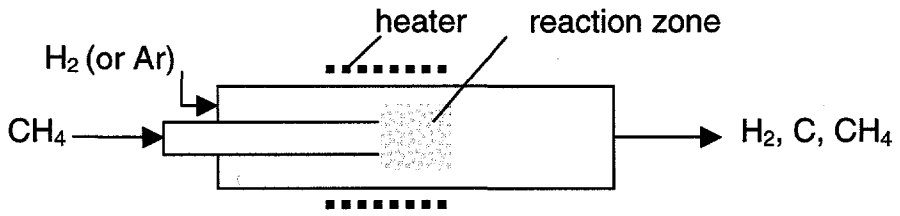

Figure 5-25. Schematic Diagram of Free Volume Reactor

There were some carbon deposits around and, especially, downstream of the reaction zone, which indicated that some portion of methane contacted the hot surface of the outer wall due to a mixing of gases in the reaction zone. This could be prevented if the temperature of a heat carrier gas was higher than that of the wall in the reaction zone. The use of an inert gas as a heat carrier requires a subsequent gas separation stage, which would add to the cost of hydrogen. On the other hand, the use of hydrogen would somewhat reduce the net hydrogen yield.

5.7.4. Fluid Wall Reactor

The objective of FWR is to carry out the high temperature hydrocarbon decomposition reactions in the layer of a carrier gas heated to the required temperature, thus preventing carbon from deposition on the reactor wall. This can be done by passing a preheated inert gas (or hydrogen) through the porous tubing (which acts as an internal reactor wall) such that it thermally decomposes methane in the reaction zone and carries away produced carbon. Simplified schematic diagram of the FWR is shown on Figure 5-26.

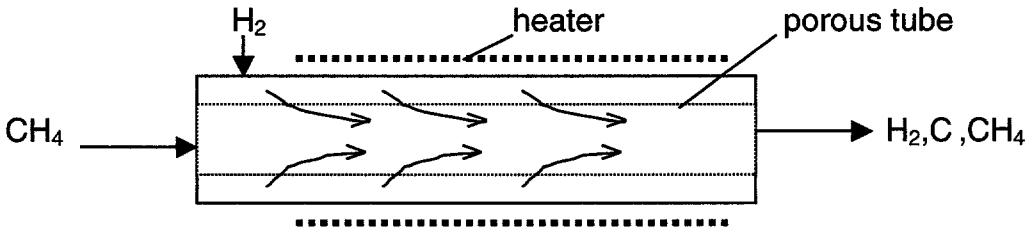

Figure 5-26. Schematic Diagram of Fluid Wall Reactor

We conducted methane decomposition test runs using small size FWR. A flow of hydrogen at positive pressure was introduced into annulus between outer tube (quartz) and the internal porous ceramic tube, and a flow of methane at the atmospheric pressure was introduced into the inner ceramic tube at H_2/CH_4 ratio of 1:3. The outer wall of the reactor was heated by the electric heater to 1100-1300°C. A stream of heated hydrogen permeated through the porous ceramic tube and entered the reaction zone where it contacted a preheated stream of methane. A mixture of hydrogen and unconverted methane after the reactor was metered and analyzed by GC method. Methane conversion was about 10-15%. Carbon was collected in the down stream trap. More experiments will be conducted to optimize the yield of products. These proof-of-concept experiments demonstrated that FWR could potentially be suitable for medium and large scale units for the simultaneous production of hydrogen and carbon from NG and other hydrocarbons.

5.7.5. Fluidized Bed Reactor

Fluidized bed reactors are widely used in chemical, metallurgical and petroleum industries. FBR could be particularly suitable for hydrocarbon decomposition process since it allows to continuously remove carbon from the reactor, similar to fluid catalytic cracking processes. A

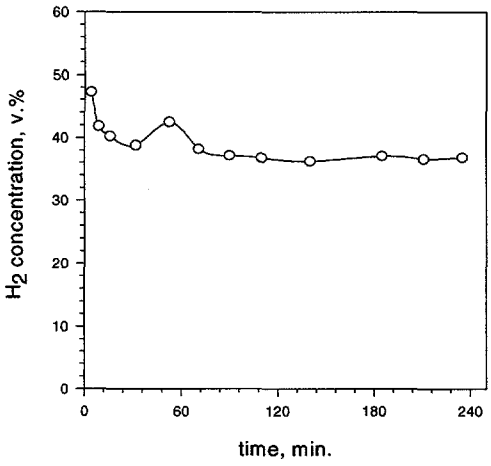

schematic diagram of FBR used in our experiments is shown on Figure 5-24 (right). It was found that an adequate fluidization of carbon (particularly, CB) particles could be achieved at space velocities of 300-600 h^{-1}. Preheated to 400-500°C a hydrocarbon stream entered the FBR from the bottom, and contacted with the fluidized bed of carbon particles heated to 850-950°C in the reaction zone, where decomposition (pyrolysis) of hydrocarbons occurred. A hydrogen-rich gas exited from the top of the reactor through a ceramic wool filter.

Figure 5-27. Catalytic Decomposition of CH_4 over BP-2000 at 950°C

FBR reactor was tested using methane, propane, methane-propane mixtures, gasoline vapor and gasoline-methane mixture as feedstocks (Figures 5-27 through 5-29). Because of relatively short residence times (approx. 1 s) in the reaction zone methane decomposition yields were relatively low, whereas, propane and gasoline were almost quantitatively converted into hydrogen-rich gas using FBR. Figure 5-28 depicts the experimental results of propane and gasoline vapor pyrolysis over CB (BP-2000) catalyst at 850°C using FBR.

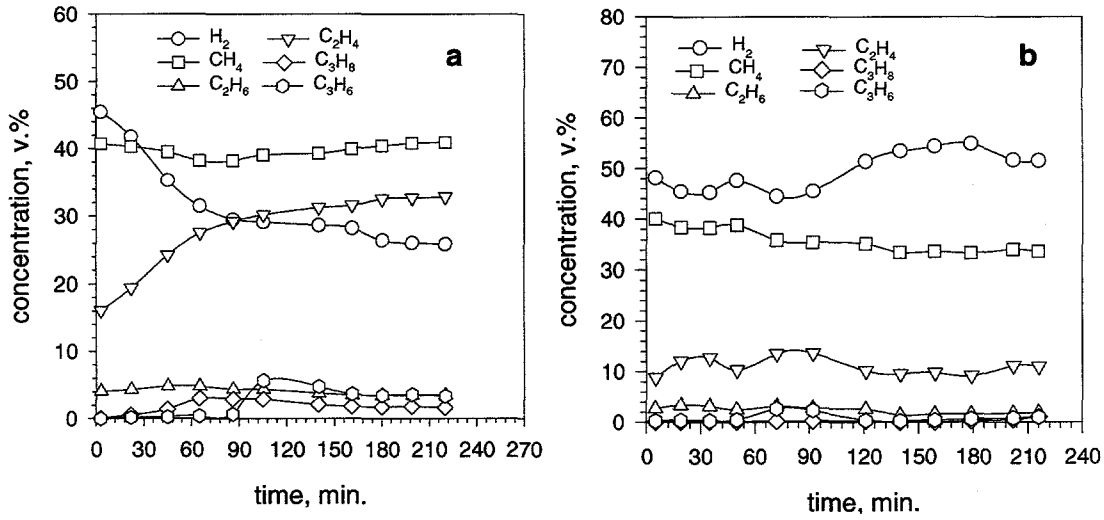

Figure 5-28. Thermocatalytic Pyrolysis of Propane (a) and Gasoline (b) over CB (BP-2000) at 850°C Using FBR

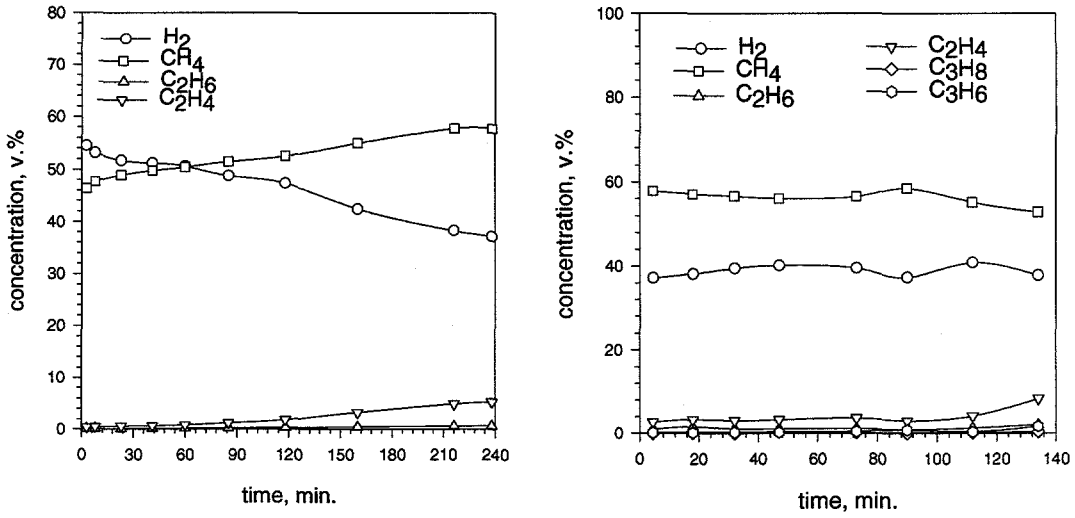

Figure 5-29. Catalytic Pyrolysis of Hydrocarbon Mixtures over BP-2000 Using Fluidized Bed Reactor: CH_4-C_3H_8 (3:1), 20 ml/min, 950°C (left) CH_4 (5 ml/min) – gasoline (1.25 ml/h), 850°C (right)

It is noteworthy that pyrolysis of propane and gasoline in FBR produce more C_2^+ byproducts comparing to PBR. Thermocatalytic pyrolysis of gasoline over CB catalyst lasted more than 3.5 hours during which the gaseous mixture with the average hydrogen concentration of 50 v.% was produced.

Figure 5-29 depict the results of pyrolysis of methane-propane and methane-gasoline mixtures over carbon black BP-2000 at 950 and 850°C, respectively, using fluidized bed reactor. The hydrogen concentration in the effluent gas was in the range of 40-50 v.%.

5.7.6. Comparative Assessment of Different Reactors for Hydrocarbon Decomposition

The results of testing of different thermocatalytic reactors for decomposition/pyrolysis of methane, propane and gasoline using carbon catalysts are presented in Table 5-3. Note that the data on the hydrocarbon conversion and the effluent gas composition relate to the average quasi-steady state values.

Table 5-3. Thermocatalytic Reactor Test Results

Hydrocarbon	Catalyst	Reac-tor	T°C	Conver-sion, %	Gaseous Products, v.%					
					H_2	CH_4	C_2H_6	C_2H_4 (C_2H_2)	ΣC_3	C_4^+
Methane	CB, BP-2000	PBR	950	30.9	47.2	52.7	0	0.1	0	0
Methane	Acetylene Black	PBR	850	23.3	37.8	61.9	0.1	0.2	0	0
Methane	CB, XC-72	PBR	850	28.0	43.7	56.2	0	0.1	0	0
Methane	CB, BP-2000	FBR	850	9.1	16.7	83.1	0	0.2	0	0
Methane	-	TR	1200	53.8	63.8	27.4	0.1	1.2 (7.5)	0	0
CH_4/H_2 (1:4)	-	FVR	1200		89.3	10.7	0	0	0	0
CH_4/C_3H_8 (3:1)	CB, BP-2000	FBR	850	38.2	50.1	2.1	9.0	0.6	0	
CH_4/C_2H_4 (3:1)	CB, BP-2000	FBR	850		36.2	53.9	2.0	7.9	0	0
Propane	AC, KE	PBR	800	100.0	88.3	11.7	0	0	0	0
Propane	Acetylene Black	PBR	850	100.0	62.1	37.9	0	0	0	0
Propane	CB, BP-2000	FBR	850	98.0	27.0	39.5	1.5	29.4	2.6	0
Gasoline	AC, KE	PBR	800	100.0	49.4	37.6	2.1	9.8	0.6	0.5
Gasoline	CB, BP-2000	FBR	850	100.0	52.0	33.2	2.1	11.1	0.7	0.9
CH_4 /gasoline	CB, BP-2000	FBR	850		40.0	55.5	0.3	3.0	0.5	0.7

AC- activated carbon
CB- carbon black
BP- Black Pearls

5.8. Characterization of Hydrocarbon Pyrolysis Products

Gaseous products of hydrocarbon decomposition/pyrolysis were identified and quantified gas-chromatographically. Hydrogen and small amounts of ethane and ethylene were major products of methane decomposition. The effluent gas of pyrolysis of propane and higher hydrocarbons contained, besides hydrogen and methane, a mixture of C_2, C_3 and C_4 alkanes and olefins which were easily identified and quantified. However the analysis of liquid products of hydrocarbon pyrolysis was much more complex. We used FTIR and UV-spectrophotometric methods for the qualitative and quantitative analysis of liquid products of propane and gasoline pyrolysis.

5.8.1. FTIR Characterization

Figure 5-30 depicts FTIR spectrum of the product of gasoline pyrolysis over carbon catalyst. The skeletal vibrations, involving C – C stretching within the ring 1595, 1494, 1441 cm^{-1}, and C – H in-plain and out-of-plain bending indicate the presence of aromatic hydrocarbons.

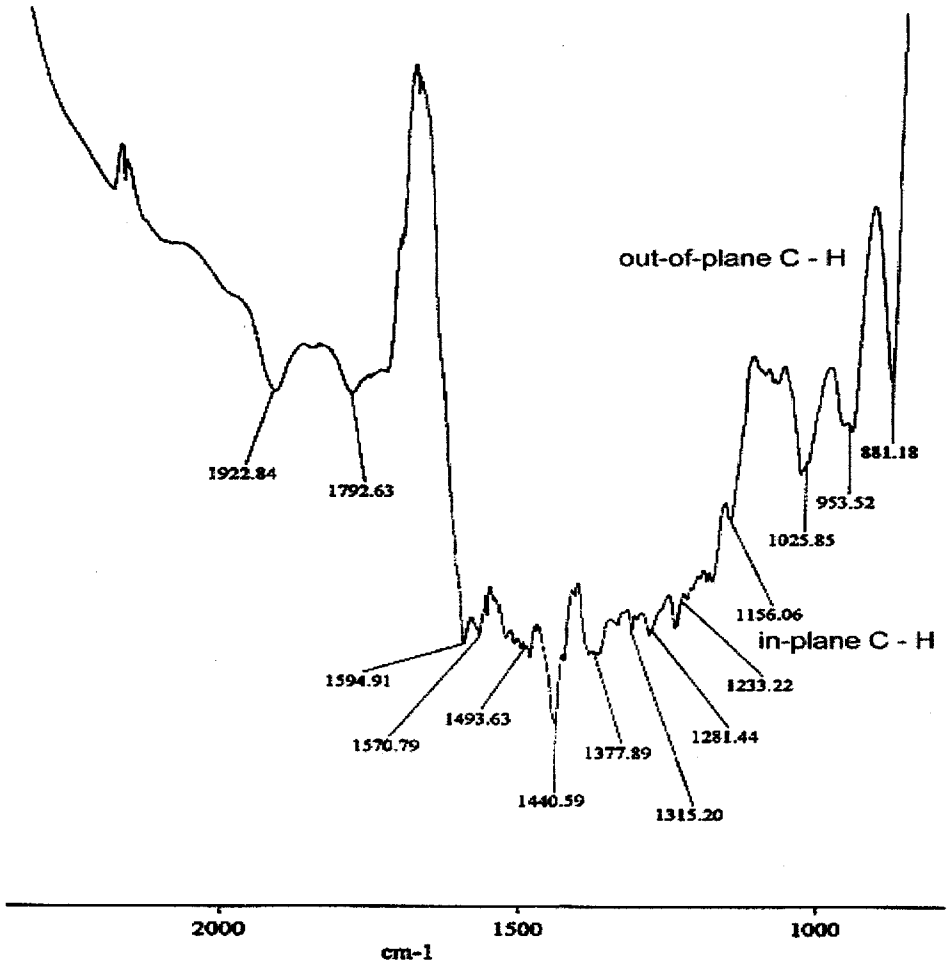

Figure 5-30. FTIR Spectrum of Liquid Product by Catalytic Pyrolysis of Gasoline over Carbon Catalyst

5.8.2. UV Spectrophotometric Characterization of Pyrolysis Products

Liquid products of hydrocarbon pyrolysis were also analyzed UV spectrophotometrically. Liquid products were condensed and collected in a collector. In most cases they represented brown-colored viscous liquids soluble in hydrocarbon-based solvents. The liquid products were quantitatively dissolved in iso-octane, diluted to the necessary concentration , filtered and placed in a special quartz spectrophotometric cuvette. UV spectra of the liquid samples were recorded by Shimadzu spectrophotometer in the range of wavelengths 200-600 nm. Figure 5-31 demonstrates UV spectrum of the liquid product produced during pyrolysis of propane over carbon black (BP-2000) at 850°C (dilution factor 12,142). The spectrum indicates a major sharp peak at the wavelength of 220 nm, and a minor peak at 250 nm, which correspond to naphthalene ($C_{10}H_8$) and anthracene ($C_{14}H_{10}$), respectively.

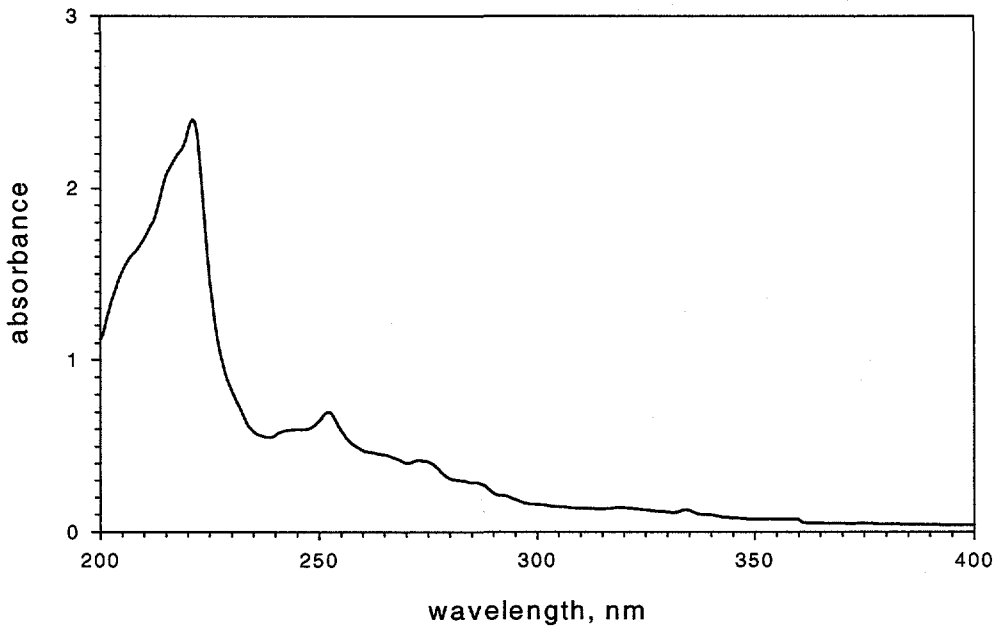

Figure 5-31. UV Spectrum of the Liquid Product of C_3H_6 Pyrolysis over BP-2000 at 850°C

The amount of naphthalene and anthracene produced were calculated based on the molar extinction coefficients (ε_{max}) and the dilution factor. ε_{max} for naphthalene and anthracene were 133,000 and 180,000, respectively. The concentration of naphthalene and anthracene in the solution can be found from *Beer-Lambert equation*:

$$Log_{10}I_o/I_t = \varepsilon Cd$$

where,
I_t and I_o are transmitted and incident light intensities,

C is the concentration of the product in solution,
D is the depth of the solution.

Based on the optical densities (A) of the solution at 220 nm (naphthalene, A=2.4) and 250 nm (antracene, A=0.7) obtained from Figure 5-31, we calculated the amount of these products produced during propane pyrolysis: 0.0033 and 0.0014 moles, respectively. Thus, the total yield of polynuclear aromatic hydrocarbons was estimated at 1.7 mol.%.

6. ECONOMIC ANALYSIS

6.1. Techno-economic Analysis

We conducted a preliminary techno-economic analysis of the thermocatalytic decomposition (TCD) process for production of hydrogen and carbon from natural gas. Figure 6-1 depicts the simplified flow diagram of the thermocatalytic process employing a fluidized bed reactor (FBR).

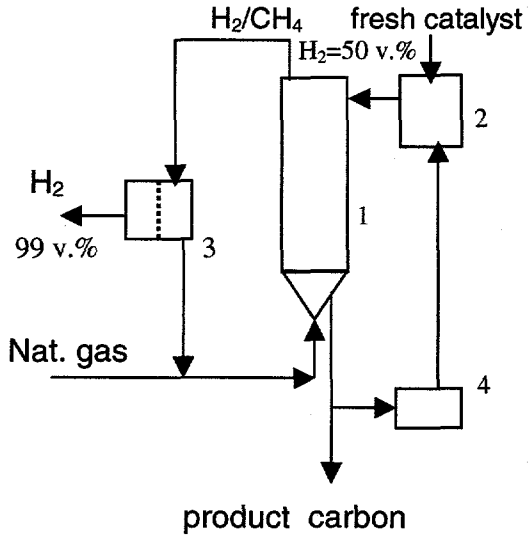

Figure 6-1. Simplified Flow Diagram of TCD Process for Production of Hydrogen and Carbon. 1- FBR, 2- heater, 3- membrane, 4- grinder

According to this flow diagram hydrogen concentration in the reactor effluent gas is 50 v.%, with balance being methane and small amounts of C_2^+ hydrocarbons. Thus, the employment of the membrane gas separation unit is required to produce 99 v.% hydrogen. Non-permeate is recycled back to the reactor. Product carbon is removed from FBR and some portion of it is ground and recycled to maintain the average particle size in the range suitable for fluidization (100 – 500 μm). The catalyst is heated in the heater to the required temperature 800-900°C. Thus, the technological scheme of the process is very close to that of fluid coking (FC) process, except, in case of FC process the temperature is lower (510-550°C), and the hydrocarbon feedstock is heavier.

Therefore, for the preliminary estimate, the capital cost of the FC plant (including grinder) and its annual operational costs were taken as a basis for the hydrogen cost estimate for TCD process (it was assumed that FC and TCD have the same capacity on a feedstock BTU basis) [34].

It was estimated that the usage of 17% of the non-permeate gas as a process fuel would cover thermal requirements for the TCD process. Carbon is a valuable byproduct of the process, with prices from several hundreds to several thousands of dollars per ton depending on its quality. Thus, the credit for byproduct carbon could significantly reduce the cost of hydrogen. For the purpose of our estimate we used a conservative sale price of carbon at $100/ton, which is the average cost of carbon (in the form of petroleum coke) used in metallurgical industry [35].

The following Table demonstrates the results of the economic evaluation of TCD plant with the capacity of 10^6 m^3/day (which is close to that of a typical steam reforming plant).

Table 6-1. Cost of Hydrogen Production by TCD Process

Capacity: 10^6 m^3 H_2/day
H_2 purity: 99.0 v.%
Natural gas: $2.5/MMBTU

	10^6	10^6/Year	$/MMBTU
Capital Cost:			
Reactor/ Heater/ Grinder (from FC plant)	18.0		
Membrane Hydrogen Separator	2.0		
Total Capital Cost	20.0		
Annual Operating Cost:			
Feedstock (Natural Gas)		33.9	
Catalyst/reagents/desulfurization		1.0	
Power		0.3	
Labor		0.1	
Depreciation (10%)		2.0	
Total Hydrogen Production Cost			7.1
Carbon Credit ($100/t)		10.7	
Net Hydrogen Production Cost			5.0

6.2. Comparative Assessment of TCD and SR Processes

Cost of hydrogen production from natural gas by thermocatalytic decomposition process was compared to that of steam reforming process. Figure 6-2 depicts the comparative assessment of TCD of NG (with and without carbon credit) and SR of NG (with and without CO_2 sequestration) processes.

For the purpose of the comparative economic evaluation we used the cost of hydrogen produced by modern methane steam reforming plant [36]. As mentioned in the Background section, capture of CO_2 from concentrated streams of SR plant and its disposal adds 25-30% to the cost of hydrogen production by SR process. One should also add to it the cost of eliminating CO_2 emissions from the diluted (stack) gases of SR process.

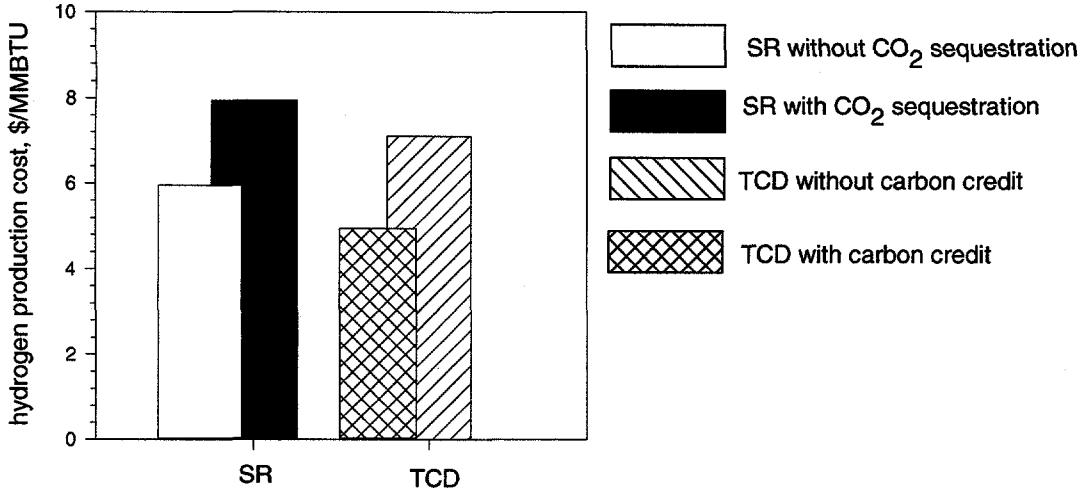

Figure 6-2. Comparative Assessment of Hydrogen Production Cost by SR and TCD Processes

The results of the comparative economic assessment of different options for hydrogen production from NG are as follows. TCD with carbon credit is the most cost effective process followed by SR without CO_2 sequestration. Note that the cost of hydrogen produced by the TCD without carbon credit (that is, carbon is not sold, but stored for the future use) is still lower than that of SR coupled with CO_2 sequestration (assuming that the cost of carbon storage is negligible compared to that of CO_2 sequestration). This is a preliminary economic assessment of TCD process, and more detailed cost analysis will be conducted upon testing pilot scale unit.

6.3. Current and Future Markets for Carbon

Currently, the total world production of carbon black is close to 6 mln tons per year, with prices varying in the range of hundreds to thousands dollars per ton, depending on the carbon quality [14]. For example, prices for the good quality carbon black could reach $1000-4000 per ton. The carbon black has a great market potential both in traditional (rubber industry, plastics, inks, etc.) and new areas. For example, [37] identified the metallurgical industry as a very promising market for carbon black. Carbon black is particularly valuable as a reducing reagent for the production of SiC and other carbides, and as a carbon additive (carburizer) in steel industry. The carbon black market for these applications in Europe currently approaches 0.5 mln ton/year with the prices for the high quality materials reaching $615 per ton. Carbon-based composite and construction materials potentially can absorb a tremendous amount of produced carbon. Besides the traditional markets for carbon, some novel applications for the carbon produced via methane decomposition are discussed in the literature. For example, Kvaerner has initiated R&D program to investigate the potential of novel grades of carbon black as a storage medium for hydrogen, and as a feedstock for the production of solar grade silicone [38].

A market for carbon-based materials is continuously growing, however, it is unlikely that all the carbon produced via NG decomposition for mitigating the global warming will be absorbed by the traditional and perspective application areas. In this case, carbon can be stored for the future

use, as discussed by Muradov [39] and Steinberg [40]. No significant energy consumption would be expected with regard to the storage of solid carbon (comparing to CO_2 sequestration).

6.4. Comparison of CO_2 Emissions from Different Hydrogen Production Processes

A comparative assessment of CO_2 emissions produced by different hydrogen production processes is shown on Figure 6-3. The following NG-based processes were compared:

- SR without CO_2 sequestration,
- SR with CO_2 sequestration,
- Plasma-assisted decomposition (PAD),
- TCD with CH_4 as a process fuel,
- TCD with H_2 as a process fuel

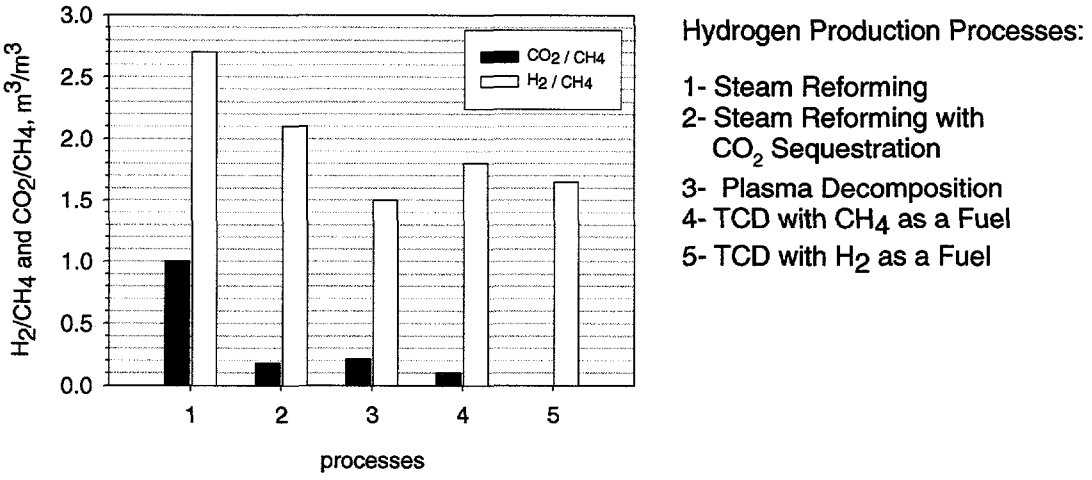

Figure 6-3. Comparison of CO_2 Emissions from Different Hydrogen Production Processes

PAD of methane is a well developed technology for the production of hydrogen and carbon black via high temperature decomposition of natural gas [38]. However, it consumes up to 1.9 kWh of electric energy to produce one normal cubic meter of hydrogen [14]. Due to relatively low endothermicity of the methane decomposition process, the thermal energy requirements of the TCD process could be covered either by 10% of methane feedstock, or 14% of hydrogen produced in the process.

The comparison is based on two parameters, which reflect the energetic and ecological features of the processes. The E_1-parameter is equal to the volume of H_2 produced from the unit volume of NG consumed as a feedstock and a process fuel ($E_1 = H_2/CH_4$ m^3/m^3). The E_2-parameter is equal to the total volume of CO_2 (from the process and stack gases) produced from a unit volume of NG ($E_2 = CO_2/CH_4$, m^3/m^3). Evidently, the higher is E_1 and lower is E_2 parameter, the better is the hydrogen production process.

The following assumptions have been made. For the sake of simplicity and comparability, it was assumed that NG was the primary fuel for the supply of both thermal and electric energy for all the processes, including PAD of NG, and for CO_2 sequestration. Almost 80% of the total world energy supply is based on fossil fuels, and NG average share is 19% [4]. Since NG produces 1.9 and 1.7 times less CO_2 (per kWh produced) than oil and coal, respectively, this assumption would result in somewhat more conservative values for CO_2 emissions. It should be also noted that the sequestration of one kg of CO_2 results in emission of 0.2-0.25 kg of CO_2 (due to large energy consumption during this process, see Section 2.2.).

The following conclusions can be extracted from Figure 6-3:

- Plasma decomposition of NG has lowest hydrogen yield and highest CO_2 emissions because of large consumption of electric energy (note that this estimate is based on the world average energy production scenario, therefore, in countries with a large non-fossil fuel energy sector, e.g. hydroelectric, nuclear energy, both E_1 and E_2 parameters could be higher and lower, respectively).
- TCD of NG (with NG as a fuel option) produces almost half of the CO_2 emissions produced by SR with CO_2 sequestration.
- TCD of NG (with H_2 as a fuel option) produces hydrogen in quantities comparable with that of SR (with CO_2 sequestration), however, it does not produce any CO_2. Thus, it is the only fossil fuel based process which shows a real potential to be a completely CO_2-free hydrogen production process.

7. SUMMARY

7.1. Summary of Results

- The technical feasibility of CO_2-free production of hydrogen via one-step thermocatalytic decomposition of hydrocarbons was demonstrated. Methane, propane and gasoline were efficiently converted into hydrogen and carbon using carbon catalysts.
- The catalytic activity and stability of more than 30 different forms and modifications of carbon were examined, and several of them were selected for further evaluation.
- The effect of operational parameters on the H_2 yield was determined. H_2 concentration in the effluent gas varied in the range of 30-90 v.%, the balance being CH_4 and small amount of C_2^+ hydrocarbons. CO or CO_2 were not detected among the products. Intermediate and byproducts of methane and propane decomposition reactions were identified and quantified.
- The factors affecting carbon catalyst activity and long term stability in hydrocarbon decomposition reactions were studied. It was found that the surface area and crystallographic structure of carbon species mostly determine the catalytic activity of carbon catalysts. This was confirmed by XRD and SEM studies of carbon catalysts.
- A kinetic model for methane decomposition over carbon catalysts was developed. Major kinetic parameters of methane decomposition reaction (rate constants, activation energies, etc.) over selected catalysts were determined.
- Various conceptual designs for the thermocatalytic reactors suitable for simultaneous production of hydrogen and carbon were evaluated. The following reactors were built and tested: packed bed, tubular, fluidized bed, free volume and fluid wall reactors.
- A bench-scale thermocatalytic fluidized bed reactor was designed and fabricated. The reactor was successfully tested using methane, propane, methane-propane mixture, and gasoline as feedstocks. Simultaneous production of hydrogen-rich gas (free of carbon oxides) and carbon was demonstrated.
- It was found that the sustainable production of hydrogen-rich gas could be attained by combination of certain type of carbon catalyst, process flow arrangement and operational conditions. Based on these experimental findings the U.S. Patent Application No. 60/194828 has been filed*
- Preliminary techno-economic assessment of the TCD process indicates that the thermocatalytic unit with the capacity of an average steam reforming plant would yield hydrogen at a cost of $5.0/MMBTU (if carbon is sold at $100/t), which is less than that for SR process. It was estimated that the TCD process compares favorably with SR coupled with CO_2 sequestration even if carbon is not sold, but stored for future use.
- Comparative assessment of CO_2 emissions from different hydrogen production processes clearly demonstrated the significant ecological advantages of the developed process over conventional processes. It was shown that the TCD is the only fossil fuel based process which shows a real potential to be completely free of CO_2 emissions.

---

* The proprietary information related to the filed patent is not included in this Report; upon request, it could be provided as a special (proprietary) attachment to the Final Report.

7.2. Publications and Patents

The following is the list of publications and patents which summarize the results of the research work accomplished under the contract.

N. Muradov, "Hydrogen from Fossil Fuels without CO_2 Emissions", in *Advances in Hydrogen Energy*, Ed. C.Gregoire Padro and F.Lau, Kluwer Academic/Plenum Publishers, New York, 2000, p.1-16

N. Muradov, "Hydrocarbon-based Systems for CO_2-free Production of Hydrogen", *13th World Hydrogen Energy Conference,* Beijing, China, 2000, p.428-433

N. Muradov, "Thermocatalytic Process for CO_2-free Production of Hydrogen and Carbon from Hydrocarbon Fuels", U.S. Patent Application, No. 60/194828, filed 04/05/2000, assignee: University of Central Florida

N. Muradov, "Thermocatalytic CO_2-free Production of Hydrogen from Hydrocarbon Fuels", *DOE Hydrogen Program Annual Review Meeting*, San Ramon, CA, 2000

N. Muradov, "Role of Hydrogen in Decarbonization of Fossil Fuels. Hydrogen from Hydrocarbons without CO_2 Emission", *Forum on Converting to Hydrogen Economy*, Fort Collins, CO, 2000

N. Muradov, "On Perspectives of CO_2-free Production of Hydrogen from Hydrocarbon Fuels for Small Scale Applications", *Symposium on Hydrogen Production, Storage and Utilization, 1999 ACS Meeting*, New Orleans, 1999

N. Muradov, "Compact Fuel Reformer for Mobile/Stationary Applications", *Summit on Miniaturization of Energy, Chemical and Biomedical Systems*, Orlando, 1999

8. REFERENCES

1. B. Cromatry, *Proceedings of the 9th World Hydrogen Energy Conference;* Paris, France, pp 13-22, 1992
2. J. Ogden, T. Kreutz, M. Steinbugler, A. Cox, J. White, *Proc. 1996 DOE Hydrogen Program Review*, 1, 125-184
3. N. Mayersohn, *Popular Science,* 66, 67-71, 1993
4. N. Nakicenovic, Energy Gases: The Methane Age and Beyond, *IIASA, Working Paper-93-033,* Laxenburg, Austria, 1-13 (1993)
5. A. Gritsenko, *Cleaning of Gases from Sulfurous Compounds,* Nedra, Moscow (1985)
6. K. Blok, R. Williams, R.Katofsky, and C. Hendriks, Hydrogen production from natural gas, sequestration of recovered CO_2 in depleted gas wells and enhanced natural gas recovery, *Energy, 22*: 161 (1997)
7. H. Audus, O. Kaarstad, and M. Kowal, Decarbonization of fossil fuels: hydrogen as an energy carrier, *Proceedings of 11th World Hydrogen Energy Conference,* Stuttgart, Germany, 525 (1996)
8. International Energy Agency. 1998. *Carbon Dioxide Capture from Power Stations.* IEA
9. M. Steinberg, and H. Cheng, Modern and prospective technologies for hydrogen production from fossil fuels, *Proceedings of the 7th World Hydrogen Energy Conference,* Moscow, 699 (1988)
10. M. Steinberg, The Carnol process for CO_2 mitigation from power plants and the transportation sector, BNL 62835, Brookhaven National Laboratory,Upton,NY, (1995)
11. A. Kobayashi, and M. Steinberg, The thermal decomposition of methane in a tubular reactor, BNL-47159, Brookhaven National Laboratory, Upton, NY (1992)
12. E. Shpilrain, V. Shterenberg, and V. Zaichenko, Comparative analysis of different natural gas pyrolysis methods, *Int. J. Hydrogen Energy,* 24: 613 (1999)
13. S. Lynum, R. Hildrum, K. Hox, and J. Hugdabl, Kvarner based technologies for environmentally friendly energy and hydrogen production, *Proc. 12th World Hydrogen Energy Conference,* Buenos Aires, 697 (1998)
14. L. Fulcheri, and Y. Schwob, From methane to hydrogen, carbon black and water. *Int. J. Hydrogen Energy, 20: 197 (*1995)
15. N. Muradov, M. Rustamov, and Yu. Bazhutin, Photoactivation of methane and other alkanes using silica-supported polyoxometalates, *Proc. Acad. Sciences USSR,* 312: 139 (1990)
16. J. Pohlenz, N. Scott, Method for hydrogen production by catalytic decomposition of a gaseous hydrocarbon stream, *U. S. Patent No 3,284,161* (UOP) (1966)
17. B. Kim, J. Zupan, L. Hillebrand, and J. Clifford, Continuous catalytic decomposition of methane, *NASA Contractor Report, NASA CR-1662*, NASA, Washington D.C.(1970)
18. M. Callahan, Hydrocarbon fuel conditioner for a 1.5 kW fuel cell power plant. *Proceedings of 26th Power Sources Symposium,* Red Bank, N.J, 181 (1974)
19. M. Pourier, C. Sapundzhiev, Catalytic decomposition of natural gas to hydrogen for fuel cell applications, *Int. J. Hydrogen Energy, 22:429* (1997)
20. K. Ledjeff-Hey, T. Kailk, J. Roes, Catalytic cracking of propane for hydrogen production for fuel cells, *Fuel Cell Seminar*, Palm Springs (1998)
21. T. Koerts, M. Deelen, R. van Santen, Hydrocarbon formation from methane by a low-temperature two-step reaction sequence, *J. Catalysis*, 138: 101 (1992)

22. F. Solymosi, A. Erdohelyi, A. Csereyi, A. Felvegi, Decomposition of CH_4 over supported Pd catalysts *J. Catalysis,* 147: 272 (1994)
23. M. Calahan, Thermo-catalytic hydrogen generation from hydrocarbon fuels. *From Electrocatalysis to Fuel Cells.* G.Sanstede, ed., Battelle Seattle Research Center (1972)
24. N. Muradov, How to produce hydrogen from fossil fuels without CO_2 emission, *Energy and Environmental Progress, Hydrogen Energy and Power Generation*, N. Veziroglu, ed., Nova Science, NY, 93 (1991)
25. N. Muradov, Hydrogen production by catalytic cracking of natural gas, *Proc. 11th World Hydrogen Energy Conference;* Stuttgart, Germany, 697 (1996)
26. A. Pyatenko, M. Nizhegorodova, V. Lipovich, V. Popov, Investigation of the process of catalytic decomposition of methane on d-metals, *Khimiya Tverdogo Topliva*, 23: 682 (1989)
27. J. Rostrup-Nielsen, Equilibria of decomposition reactions of carbon monooxide and methane over nickel catalyst, *J. Catalysis,* 27: 343 (1972)
28. A. Steinfeld, V. Kirilov, G. Kuvshinov, Y. Mogilnikh, A. Reller, Production of filamentous carbon and hydrogen by solar thermal catalytic cracking of methane, *Chem. Eng. Sci.* 52: 3399 (1997)
29. E. Shustorovich, The bond-order conservation approach to chemisorption and heterogeneous catalysis: applications and implications, *Advances in Catalysys*, 37:101 (1990)
30. A. Frennet, Chemisorption and exchange with deuterium of methane on metals, *Catal. Rev.- Sci. Eng.,* 10: 37 (1974)
31. Diefendorf, R. 1960. *J. Chem. Physics,* 57, 3, 815
32. A. Tesner, *The Kinetics of Carbon Black Production;* VINITI: Moscow (1987)
33. C. Chen, M. Back, R. Back, Mechanism of the thermal decomposition of methane, *Symp. Industrial and Laboratory Pyrolysis,* (1976)
34. D. Garrett, *Chemical Engineering Economics.* New York: Van Nostrand Reinhold, 1989
35. *Kirk-Othmer Encyclopedia of Chemical Technology.* V. 4. New York: John Wiley & Sons, 1978
36. J. Ogden, M. Steinbugler, and T. Kreutz. "Hydrogen as a Fuel for Fuel Cell Vehicles: a Technical and Economic Comparison." In *Proceedings of the *th Annual U.S. Hydrogen Meeting,* 469. Alexandria, VA: NHA, 1997.
37. B. Gaudernack, and S. Lynum. "Hydrogen from Natural Gas without Release of CO2 to the Atmosphere." In *Proceedings of 11th World Hydrogen Energy Conference,* Stuttgart, Germany, 511-523, 1996.
38. S. Lynum, R. Hildrum, K. Hox, and J. Hugdabl. "Kvarner Based Technologies for Environmentally Friendly Energy and Hydrogen Production." In *Proceedings of 12th World Hydrogen Energy Conference, 697.* Buenos Aires, Argentina, 1998
39. N. Muradov, "How to Produce Hydrogen from Fossil Fuels without CO_2 Emission." *Intern. J. Hydrogen Energy,* 18: 211, 1993
40. M. Steinberg, "Fossil Fuel Decarbonization Technology for Mitigating Global Warming." *Intern. J. Hydrogen Energy,* 24: 771, 1999.